ROLL HARDNESS MEASUREMENT

By

PAUL O. PADGETT

Bachelor of Science in Mechanical Engineering

Oklahoma State University

Stillwater, Oklahoma

1985

Submitted to the Faculty of the Graduate College
of the Oklahoma State University
in partial fulfillment of the requirements
for the Degree of
MASTER OF SCIENCE
December, 1986

ROLL HARDNESS MEASUREMENT

Thesis Approved:

R L Lowery
Thesis Adviser

J. K. Good

Gary E. Young

Norman N. Durham
Dean of the Graduate College

ACKNOWLEDGMENTS

I would like to express my appreciation to all of those who have assisted me in this study. Special words of appreciation are extended to Dr. R. L. Lowery, my thesis adviser, for his guidance, encouragement, and optimistic outlook throughout the course of this research work. I would also like to thank Dr. J. K. Good and Dr. G. E. Young for their participation as committee members.

I am very grateful to my wife, Sherri, for her assistance and patience while I pursued my academic goals. I am also grateful to my parents for their encouragement and inspiration.

Finally, I would like to express my appreciation to Ms. Charlene Fries for her outstanding work in preparing this manuscript.

TABLE OF CONTENTS

LIST OF TABLES

LIST OF FIGURES

Figure Page

LIST OF SYMBOLS

A	pressure amplitude of acoustic waves
b	wave propagation constant
B	bending stiffness
C_a	acoustic velocity in air
C_b	propagation velocity of waves in a panel
C_L	longitudinal wave velocity
C_p	wave velocity in a roll
E	Young's modulus
$\bar{f}$	force
f_c	coincidence frequency
$f_{n,m}$	frequency associated with the mth and nth mode of vibration of a panel
f_o	resonant frequency
j	imaginary unit
L	linear distance
P	acoustic pressure
r	characteristic impedance
R	reflection ratio
R_I	intensity reflection coefficient
t	web thickness
T_I	intensity transmission coefficient
T.L.	transmission loss

$\bar{V}$	velocity
$\bar{Z}$	acoustic impedance
$\bar{Z}_m$	mechanical impedance
ρ_a	air density
ρ_p	web density
σ	surface density
ω	angular frequency

CHAPTER I

INTRODUCTION

Overview

There is a considerable need in the web handling industry for a system or device which can accurately determine the hardness of a roll of web material. In particular, the device should be able to make the hardness measurement while the roll is being formed. Since roll hardness varies along the length of the roll, the transducer should be portable enough to allow mounting in a traversing carriage. In most cases it is acceptable for the transducer to make contact with the roll; however, in some cases, such as a coating process, it is mandatory that the transducer not contact the roll. It is the latter situation where the need is especially evident. In this study both contacting and noncontacting methods will be discussed. The major emphasis will be on a noncontacting method using the reflections of acoustic waves from the roll.

The units that roll hardness are measured in will depend upon the measuring system used. For example, if a force hammer and accelerometer are used, the units could be Ns/m; if the measurement system uses acoustic reflections, the units might be a reflection intensity or reflection ratio, both of which are dimensionless. Of course, this is not important because what will actually be determined is: how hard or soft is the roll compared to some standard.

The importance of roll hardness in the overall process of manufacturing thin flexible materials, conditioning the materials by coating, slitting, printing, etc., or in the handling of rolls between processes or as a finished product cannot be understated. Frye [1] mentions a study conducted by Beloit Corporation and Lennox Machine Company which found 300 different types of roll defects in rolls of paper and identified the causes. Over 87 percent of these defects originated or were magnified during the forming of the roll. A few of the more important defects caused specifically by the winding process are starring, telescoping, snapoffs, and bagging. Starring and telescoping usually originate in rolls which have been wound too softly. Hard rolls may cause snapoffs (web breakage during an unwinding process) or bagging due to excessive wound in tension.

Literature Survey

Several methods for measuring roll hardness are mentioned in the literature; however, all of these methods require physical contact with the roll. These methods may be categorized as static or dynamic. A static method is one which requires the motion of the roll to cease before reading can be taken; thus, a static cannot be incorporated in a process control environment. They are useful in making occasional adjustments in the winding machine or in research. Dynamic methods can be used to measure roll hardness while the roll is turning and taking on new material.

Static Methods for Determining Roll Hardness

The Cameron Strain Test [2] is usually performed when the roll is

completely finished. The procedure is to cut the outer ply across the full width of the roll. The resulting gap between the two cut edges is then measured. This gap distance is divided by the circumference of the roll, multiplied by 100, and called the strain factor. The strain factor is used to predict the probability of the web snapping off during an unwinding process. The accuracy of the prediction requires historical evidence of the performance of other rolls and their corresponding strain factors. This method is time consuming and requires a lot of manpower, not to mention the fact that it is destructive.

The Schmidt Concrete Test Hammer [3] method uses the rebound height of a mass impacting the roll to indicate hardness. This test, after proper calibration, provides a numerical value for the roll hardness that must be compared to a standard hardness number to indicate if the roll is too hard or too soft. The drawback of this method, aside from being static, is that strict adherence to the test procedures is required for consistent results.

Pfeiffer [4] discusses, qualitatively, three procedures for measuring roll hardness. In the first method, microphones were used to record the sound waves produced by a hardwood club striking a roll. Spectrum analysis was then performed on the recorded signal to locate the resonant frequencies. Although skilled operators could determine the roll condition from the sound produced, no correlation was found between the processed signal and roll hardness. In the second method, a steel bar--outfitted with an accelerometer--was dropped onto the roll. The peak acceleration was used to indicate hardness. Harder rolls produce a higher peak acceleration and shorter contact duration. The final method discussed uses the speed of sound through the layers of the roll to indicate

hardness. A sound source is placed in the core of the roll and a receiver is used to pick up the transmitted waves at various locations along the radius of the roll. The measurand is the time interval between transmission and reception of the acoustic signal. Faster times correspond to harder rolls. Commercial application of this method will be a problem, due to the placement of the sender and receiver.

Welp and Schoenmeier [5] wound thin steel strips laterally, with the end of each strip protruding from the roll edge, into rolls of paper. The force required to pull the strips out was used as an indication of roll hardness. They report that the pressure between the layers of the finished roll is a good indicator of roll hardness. A similar method using nylon tabs was used by Monk, Lautner, and McMullen [6]. These methods are primarily used by researchers studying internal roll structure.

The J-line method gives an indirect indication of roll hardness. A radial line is drawn on the edge of the roll after a sufficient depth of layers has accumulated (usually a few inches). The winding is then allowed to resume. As the roll builds the line deforms into a J shape as layers slip relative to one another. Soft rolls cause more deformation than hard ones. This method is discussed by several authors (Welp and Schoenmeier [5], Frye [7], and Laumer [8]).

Dynamic Methods for Determining Roll Hardness

Ericksson, Lydig, and Viglund [9] describe a system for on-line measurement of roll density. Roll density is synonymous with roll hardness. The apparatus consists of two equal diameter drums which ride on the roll. A transmitter on one of the drums sends a pulse for each revolution of the roll while a transmitter on the second drum sends a pulse for each

revolution of the drums. The pulses are processed by a computer which calculates the circumference of the roll each time a new layer of web is added. Knowledge of the web density allows computation of the roll density. Of course, higher densities correspond to harder rolls. McDonald and Farrell [10] studied a similar system; the only difference was that they used a transmitter mounted on the roll shaft to count roll revolutions. These systems are mainly used on winding machines that power the roll through the roll surface (surface winding).

Duff [11] discusses the use of a transducer called the Backtender's Friend to measure roll hardness. The transducer consists of a piezoelectric crystal mounted on a disc. The disc rolls on the surface of the roll and each time the crystal contacts the roll, a voltage proportional to the roll hardness is produced. A traversing mechanism, which supports the sensor, allows hardness readings to be taken over the entire length of the roll. There is a problem associated with high speed operation in that unless the roll is perfectly smooth, the transducer will bounce and produce erroneous readings.

A system which measures roll caliper (diameter) is described by Quint [12]. Although this system does not measure roll hardness, it can be used to indicate hard or soft areas in a particular roll. The apparatus consists of a small diameter cylinder mounted vertically in a traversing carriage. Output is roll diameter as a function of position along the length of the roll. Larger diameters correspond to soft areas. High speed operation with this system would be difficult.

An additional transducer, called the Rho-Meter, was noticed in an advertisement [13]. The manufacturer, Beloit Eastern Corporation, could not be contacted; thus, no technical information was located. The Rho-

Meter is mentioned in passing by Pfeiffer [4], Frye [7], and McDonald and Farrell [10]. It is speculated that it is based on a type of hammer mechanism.

Statement of Problem

This study will discuss the problems associated with two different methods of measuring roll hardness. One of the methods will incorporate a force hammer and accelerometer; thus two signals will be produced. It is desired to determine which part of the information contained in the signals can be used to obtain an indication of hardness. The second method will utilize the reflections of acoustic waves from the roll surface to sense the hardness. Of particular interest is the behavior of the waves as they are reflected from the roll. The possibility of measuring the air space between the roll and one loose layer will also be explored. The operating frequencies which yield the optimum measurability and repeatability will also be determined.

Approach to the Problem

The portion of this study concerned with the force hammer accelerometer system will utilize a small winding machine to produce rolls of varying hardness and a digital waveform analyzer to record and process the force and acceleration signals. The two signals will be analyzed in the frequency domain by a Fast Fourier Transform (FFT) algorithm. The position of the dominant frequencies will be studied with respect to their correlation to roll hardness. Time domain analysis will be conducted to determine the peak force and peak acceleration characteristics of the signals and their correlation to roll hardness.

The portion of this study concerned with the acoustic reflection measurement system will discuss experiments performed to determine the transmission properties of thin, flexible membranes. Knowledge gained with these tests will be used to develop a simple model of a roll with one loose layer. The characteristics of this model will be analyzed theoretically to determine phenomena on which a roll hardness measuring system could be based. Experiments will be performed in an attempt to verify the model. The frequency range is limited to less than 20 kHz. Both the theoretical and experimental work will use paper as the web material; however, extrapolations to other materials will be discussed.

Organization

Chapter II will discuss the force hammer-accelerometer system and present the results of tests conducted on rolls of different hardness. Chapter III describes the procedures and equipment used to carry out transmission phenomenon tests on thin, flexible panels and presents the experimental results. In Chapter IV a model of a roll of web material with one loose layer is developed and discussed. Chapter V presents experimental verification of the model described in Chapter IV. Conclusions and recommendations will be presented in Chapter VI.

CHAPTER II

ROLL HARDNESS MEASUREMENT USING A FORCE IMPULSE

Many roll hardness measurement techniques are based on the concept of inputting a force impulse into the roll and analyzing the response. Workers sometimes whack rolls with a wooden stick as the rolls are being wound. The sound produced is the response. Human judgment is required in this case to determine how well the roll is being wound. The accelerometer outfitted steel bar, as described by Pfieffer [4], inputs a force into the roll when it is dropped. The acceleration of the bar is the response. The restriction here is that the bar must be released from exactly the same distance from the roll if peak acceleration is used as the criteria. This is not unlike the Schmidt Hammer Test [3], except the response in this case is the rebound height.

In this part of the study, the goal was to develop a method that could utilize the response of an arbitrary force impulse input to make the hardness measurement. The approach was entirely experimental.

Experimental Procedure

A small winding machine was built for the sole purpose of winding rolls of various hardnesses. The winding tension was the variable used to quantify the roll hardness. The tension applied to the web was held constant while the roll was being wound and the winding was done slowly so that air entrainment was not a factor. Therefore, when tests were

performed on the rolls, the results were analyzed with respect to the web tension under which the roll was wound. Higher tension implies a harder roll. The web materials used were polypropylene and paper.

The other equipment used in these tests included an impulse force hammer, accelerometer, and a DATA 6000 Digital Waveform Analyzer manufactured by the Data Precision Division of the Analogic Corporation. The force transducer and accelerometer were attached via a small stud screw so they essentially become a single unit, similar to an impedance head. The waveform analyzer has a maximum sampling rate of 100 kHz when one channel is used, and 25 kHz when more than one channel is used. Since the force and acceleration signals were both being recorded, the maximum sampling rate of 25 kHz was used. The waveform analyzer also allows pre-trigger points to be retained in the record; this insures that the entire transient will be captured.

The onboard computer of the waveform analyzer is capable of performing a wide range of mathematical manipulations. This allows a detailed analysis of the waveforms. The mechanical impedance at the driving point of the roll is given by

$$\bar{Z}_m = \frac{\bar{f}}{\bar{v}} = \frac{\text{force}}{\text{velocity}} \qquad (1)$$

Since the output signals are force and acceleration, the acceleration signal is integrated to yield the velocity. In implementing Equation (1) with the waveform analyzer, there is a slight problem of dividing the force signal by small velocity values near the origin. The important parts of the impedance curve are lost because of the large values near the origin. Thus, the first step in the signal processing is to delete the first few values from each data set and begin the point

division at some later time. The mechanical impedance of the roll was also analyzed with respect to its Fourier Transform using the FFT algorithm on the waveform analyzer.

The question of accuracy must also be addressed. Doebelin [4] states that the force transducer may be modeled as a spring sandwiched between two end masses. The measured force is the force in the spring. He suggests the criteria for accurate measurement is

$$\frac{F_m}{F}(D) = \frac{MD}{Z(D)} + 1 \qquad (2)$$

where F_m is the measured force, F is the actual force in the roll, M is the mass between the piezoelectric crystal and the roll, and D is the differential operator. Thus, the force input into the roll must be large enough to ensure that the ratio in Equation (2) is close to unity. Accurate acceleration measurement is ensured if the spring between the two masses is stiff enough. The modulus of elasticity of piezoelectric crystals is on the order of 10^{10} N/m^2, which suggests that the spring constant is very large.

The steps involved in the experimental procedure are now outlined. After a roll is wound and the tension noted, the roll is struck with the force hammer. Excellent force and acceleration signals can be obtained by essentially letting the hammer fall onto the roll. The peak voltages and time duration of each signal are noted. Integration of the acceleration signal is then performed, a fixed number of initial points deleted from each data set, and the result of Equation (1) stored in a new data set. The FFT of the mechanical impedance is then taken.

Experimental Results

Figures 1 and 2 show the force and acceleration signals obtained by striking a hard roll (winding tension of 90 N/m) and a soft roll (winding tension of 45 N/m), respectively. The response is exactly as expected: the peak force and acceleration are higher and the time durations are shorter for the hard roll. Neither the peak acceleration or force nor the time durations taken by themselves can be used in a system where the force is arbitrary. Also, the ratio of the peak force to peak acceleration is always approximately equal; this is a reasonable finding according to Newton. However, if the peaks are considered with respect to the time duration, they yield a usable variable. Consider the acceleration signal; if the force input to a soft roll is high enough, the peak acceleration could easily be as high as the peak acceleration for the hard roll but the time duration would be considerably longer. Thus, for an arbitrary force input, the ratio of the peak acceleration to the time duration is always larger for a harder roll. Applying this rule to the acceleration signals of Figures 1 and 2 yields values of 770 volts per second for the hard roll and 160 volts per second for the soft roll. Good resolution is clearly possible, and the force need not be measured.

Figure 3 shows the mechanical impedance of the hard and soft rolls. Equation (1) was applied after deleting the first 12 points from the force and velocity data sets; this is equivalent to a time shift of 0.48 milliseconds. The shape of each curve is strikingly similar and actually they yield no new information. The only generalization that can be made is that the slope is always greater for hard rolls than for soft rolls. This fact is the result of the increased damping present in the

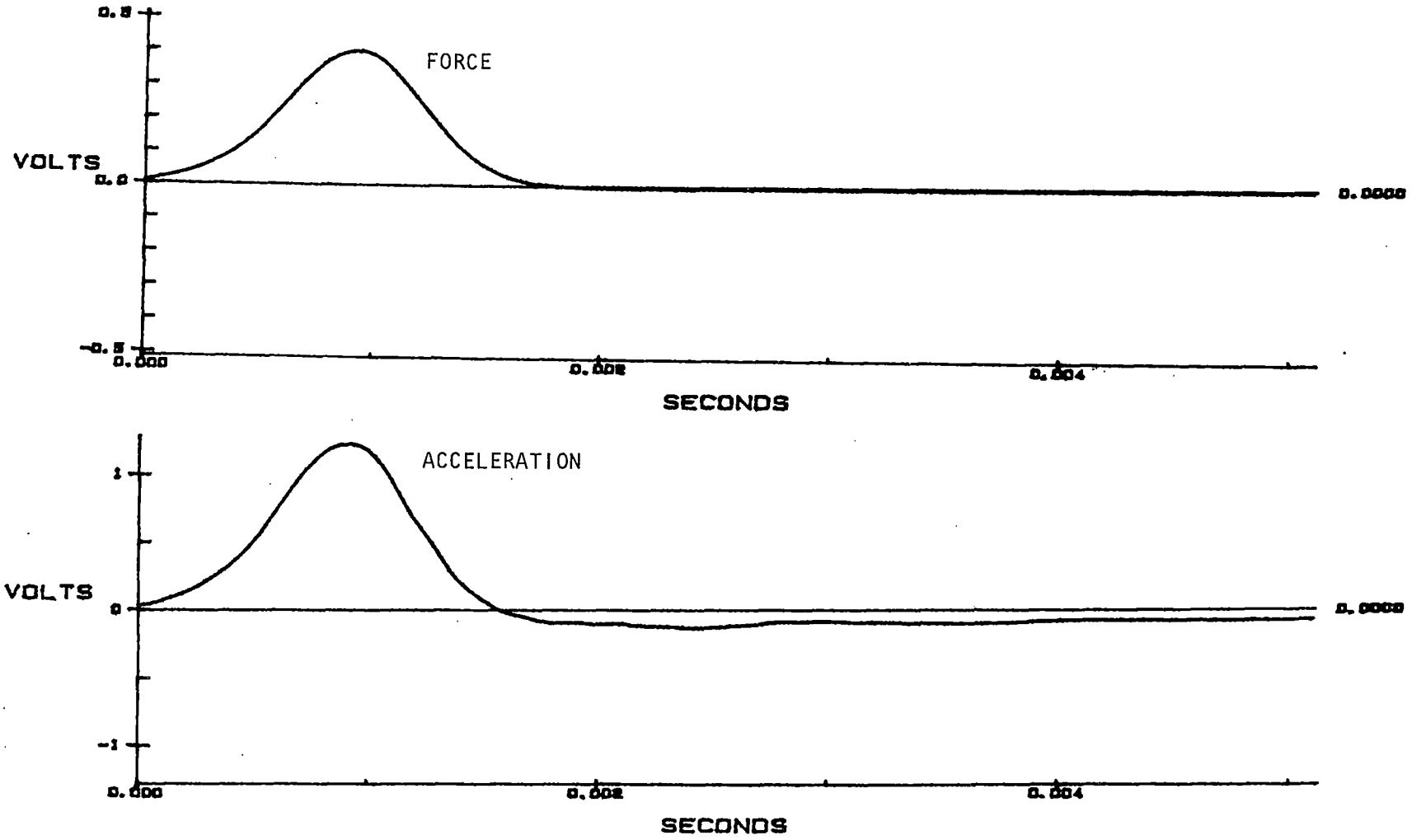

Figure 1. Force and Acceleration Signals Taken From a Hard Roll

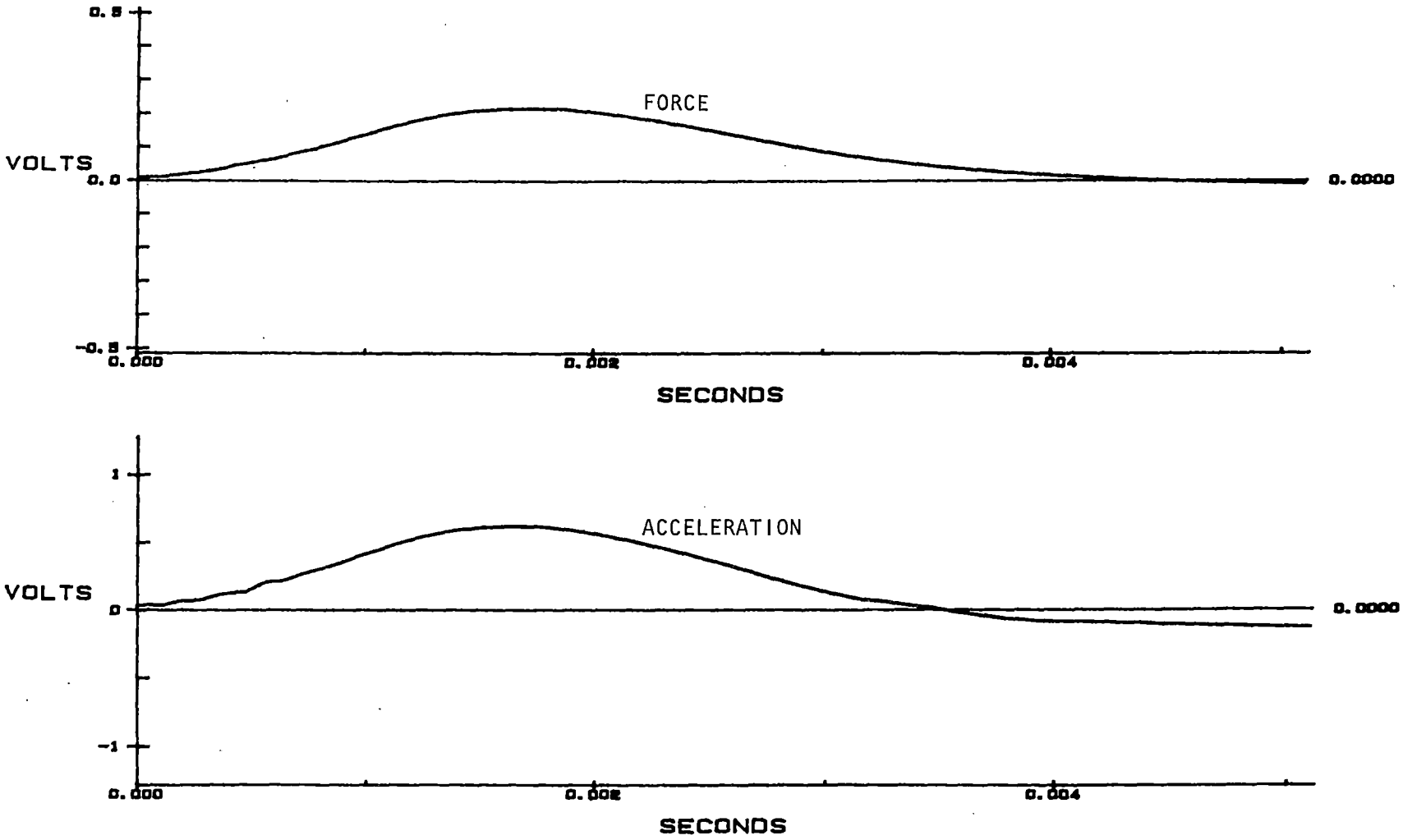

Figure 2. Force and Acceleration Signals Taken From a Soft Roll

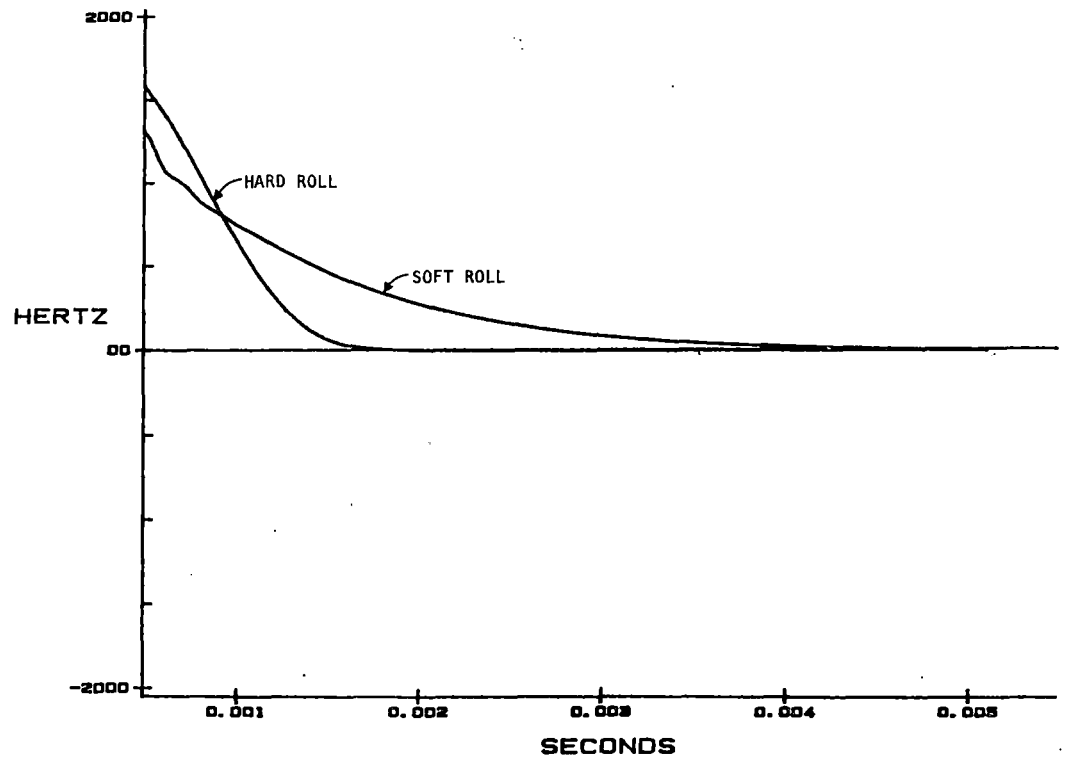

Figure 3. Comparisons of the Mechanical Impedances of a Soft and Hard Roll

soft roll. This is evidenced further by considering the magnitude of the coefficients given by the FFT of each of the mechanical impedance curves as shown in Figure 4.

The natural frequencies are higher in the hard roll because of less damping. Note that the peak in the magnitude curve occurs at a higher frequency for the hard roll. Also, the higher rate of decay evident in the mechanical impedance curve for the hard roll points to the fact that, relative to the soft roll, the peak in the magnitude curve should be lower; this is in fact the case. Thus, it is probably true in general that the FFT curve should be less in magnitude and the maximum occur at a higher rate in frequency for harder rolls. However, there is insufficient experimental evidence to make definite conclusions about the frequency content of the mechanical impedance of the rolls.

During the tests an anomaly was observed which deserves mentioning. For small rolls (those containing only one or two inches of web layers) two peaks were evident in the force and acceleration signals. It is speculated that the force causes a pressure wave to propagate through the roll which, upon encountering the large impedance discontinuity at the core, is reflected back to the force transducer. Thus, the first peak corresponds to the actual peak force and the second peak is due to the reflected pressure wave. The reason this is not evident in the larger rolls could be due to attenuation or a longer travel time. Another plausible explanation is that the low mass of a small roll allows excitation of the supporting structure. Further investigation is needed to determine the exact cause.

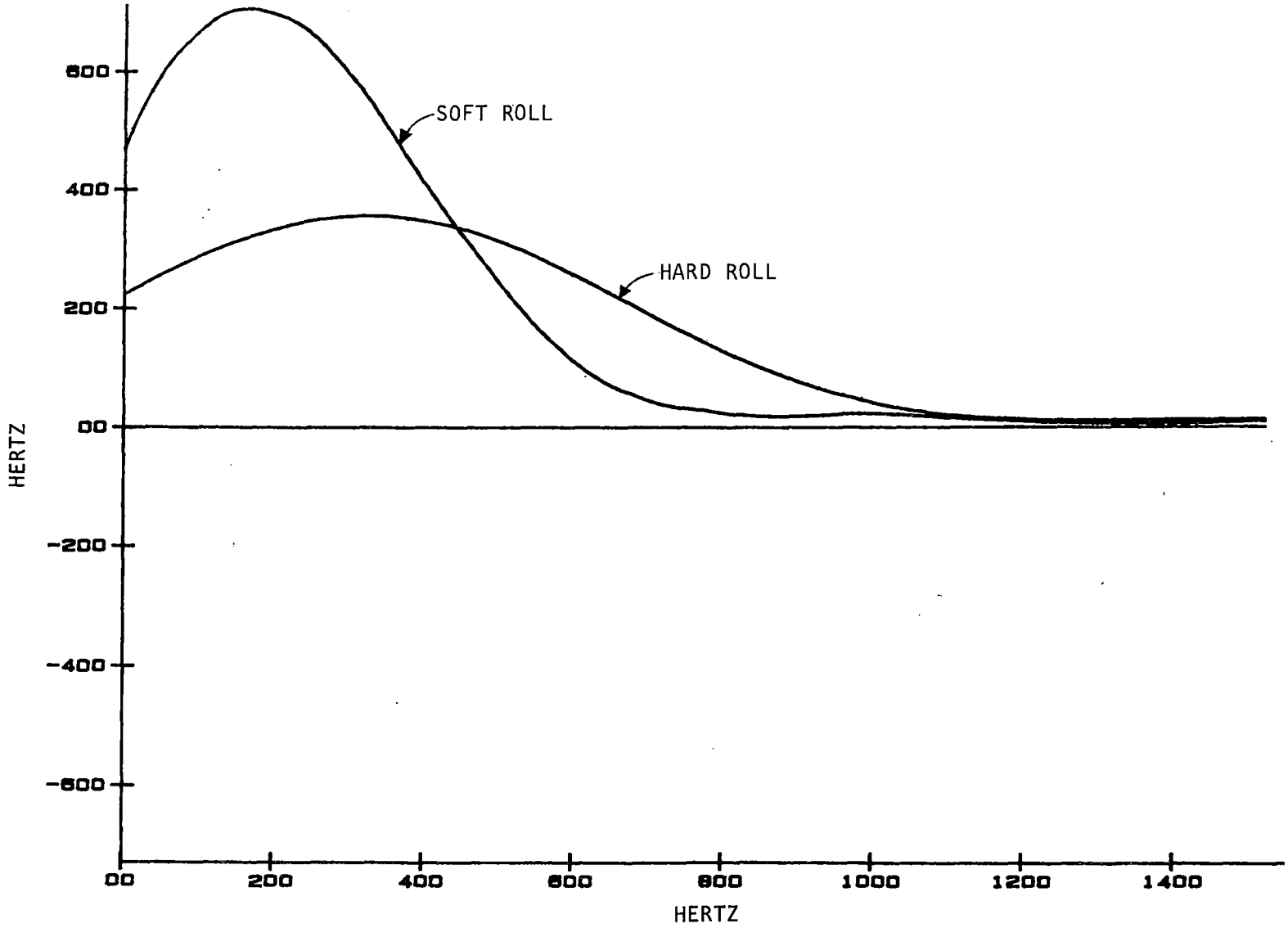

Figure 4. Frequency Spectra of the Mechanical Impedance Curves

Applications

In the previous section, three quantities were discussed which provide information about the roll hardness: the ratio of the peak acceleration to the duration time, the slope of the mechanical impedance curve, and the frequency at which the peak in the spectrum of the mechanical impedance of the roll occurs. In actual application the necessary signal manipulation would have to be carried out electronically or with a computer. Consider the acceleration time ratio. All that is required would be a mass-accelerometer system. Of course, a "standard" ratio would be needed for comparisons. A standardized "hit" would not be necessary. The sequence of events would be to strike the roll, process the signal to determine the peak acceleration and duration time, carry-out the division, and compare the result to the standard. If the system was operated manually, a certain range of tolerance would need to be placed around the standard ratio. The output could then be displayed to tell the operator if the roll was winding properly. Automatic operations could be done by mounting the transducer in a traversing carriage. The possibility then exists for the computer to subtract the acquired ratio from the standard. The resulting error signal could be used by a control algorithm to initiate adjustment in the tension or nip pressure.

Problems relating to the small diameter roll during startup with respect to the previously mentioned anomaly will have to be considered. In addition, there is the transverse loading problem on the transducer when measurements are taken from a moving roll.

CHAPTER III

TRANSMISSION LOSS THROUGH THIN PANELS

It was originally thought that an acoustic wave reflected from a soft roll would appear attenuated when compared to a wave reflected from a hard roll. Tests were carried out on hard and soft rolls by impacting the rolls with acoustic pulses and monitoring the reflections. The reflections from the soft rolls were in fact attenuated, but the attenuation was much too small for practical application. The difference in the characteristic impedance between a soft roll and a hard roll is too slight when compared to the characteristic impedance of air. The frequencies used ranged from 5 to 20 kHz but none produced the desired result.

Since the differences in the reflections from hard and soft rolls were so small, a different procedure was tested. The acoustic wave reflections from a tightly wound roll and a tightly wound roll with the outer plys loosened up were analyzed. The results of this series of tests showed that there was very little difference in the reflections. Figure 5 shows an example reflection comparison taken from a hard roll with four loose wraps; the frequency was 20 kHz. From the figure it can be seen that the attenuation is very small, and this is one of the better examples. Since it was not known if the waves were being reflected by the first layer or if some penetration was occurring, it was decided to do some experimental work on the transmission phenomena of thin membranes.

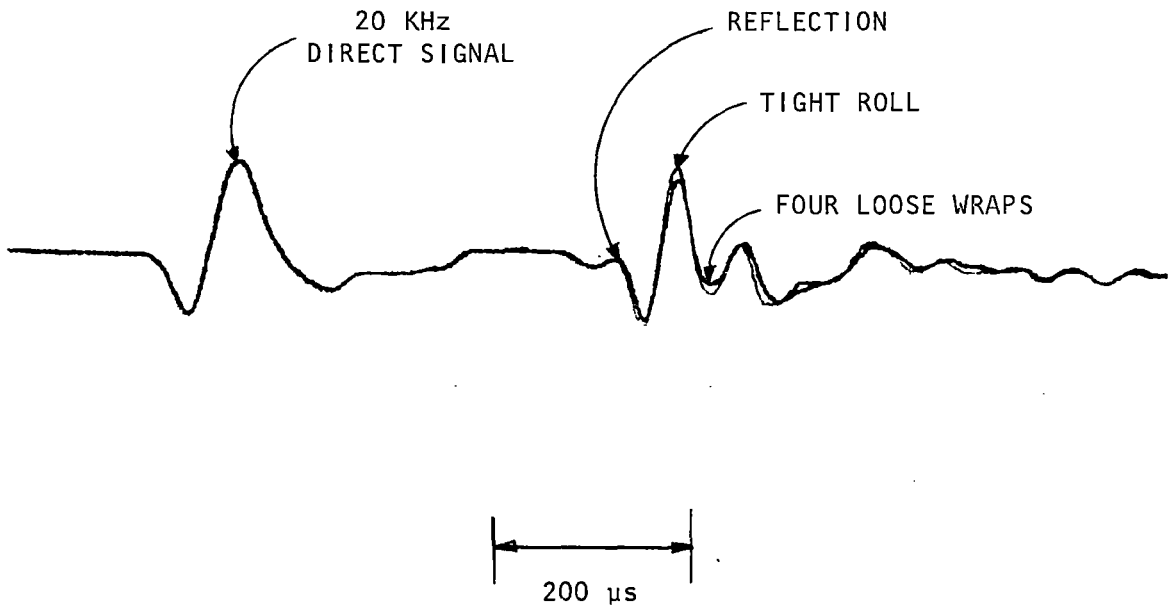

Figure 5. Comparisons of Reflections Taken From a Hard Roll and Hard Roll With Four Loose Wraps

Experimental Procedure

Figure 6 shows the experimental apparatus used in this part of the study. The tone burst generator allows a selected number of cycles from the oscillator to proceed to the amplifier and speaker. A continuous wave could have been used, but a measurement system based on reflections will necessarily have to be pulsed. Thus, it was decided to use pulses here. The high frequencies, up to 20 kHz, prompted the use of a digital waveform recorder. This recorder has one channel, a 10-bit analog to digital converter, and a maximum sampling rate of 2 MHz. After capturing the transient the recorder plays the signal back at 10 points per second to a Y-T plotter. The waveform recorder was triggered by the signal sent to the speaker.

A number of wavetrain lengths were tested. Using only one or two cycles in the wavetrain, the measured frequencies did not correspond well with the input frequency. From three or more cycles on the correspondence was much better. It seems that the speaker needs time to overcome transients because of the inertial resistance offered by the voice coil when it is standing still. A four-cycle pulse train was chosen for the experiments.

A sequence of measurements was taken at each frequency. The direct signal was recorded first, then the pulses transmitted through one, two, and four sheets were recorded (Figure 7). The amplitudes of the third cycle were measured and the transmission loss computed from

$$\text{T.L.} = 20 \log \left(\frac{A_{1,\ 2,\ \text{or}\ 4}}{A_o} \right) \text{(dB)} \qquad (3)$$

where A is the amplitude of the signal at the third cycle and the sub-

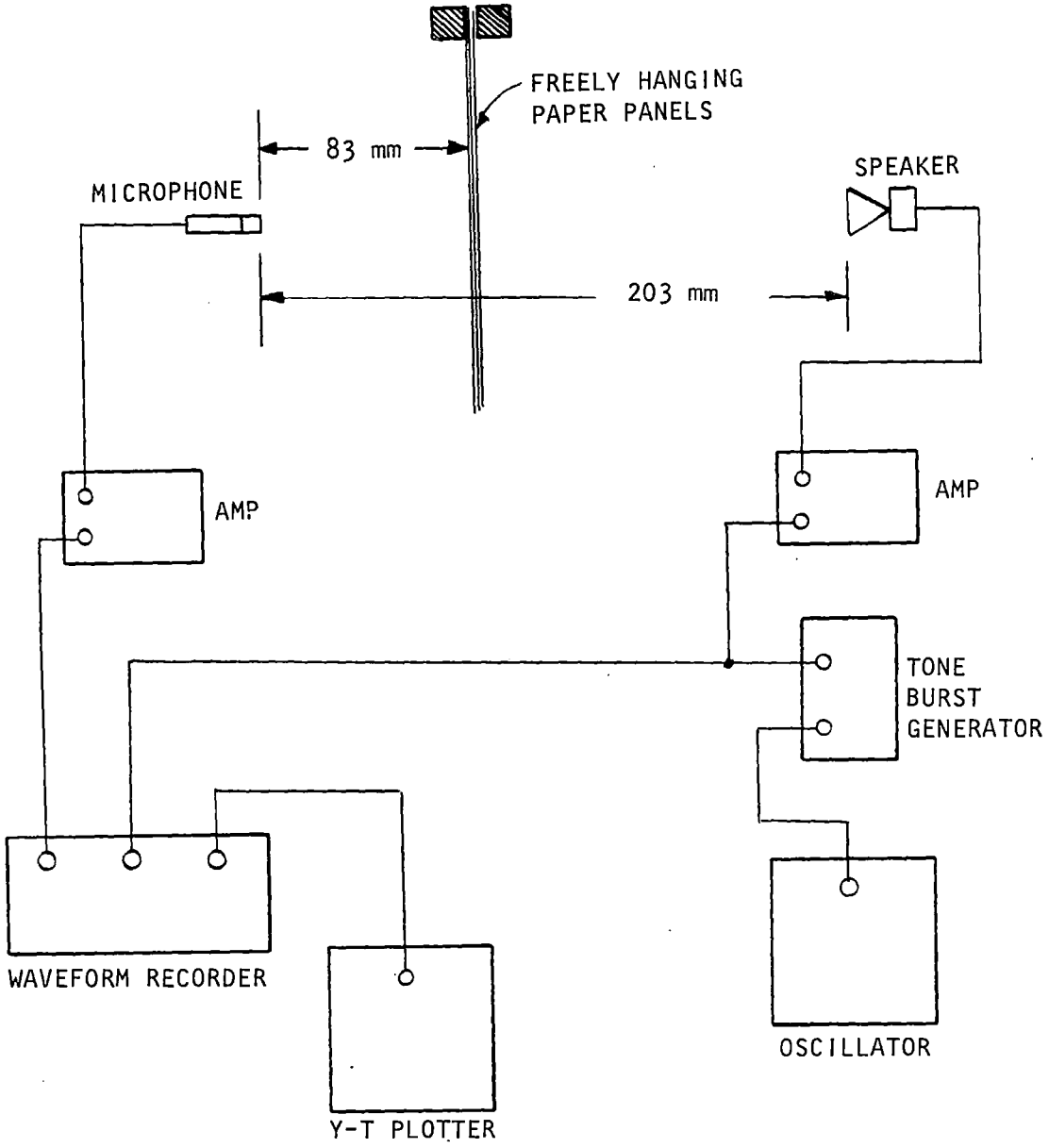

Figure 6. System for Making Transmission Loss Measurements

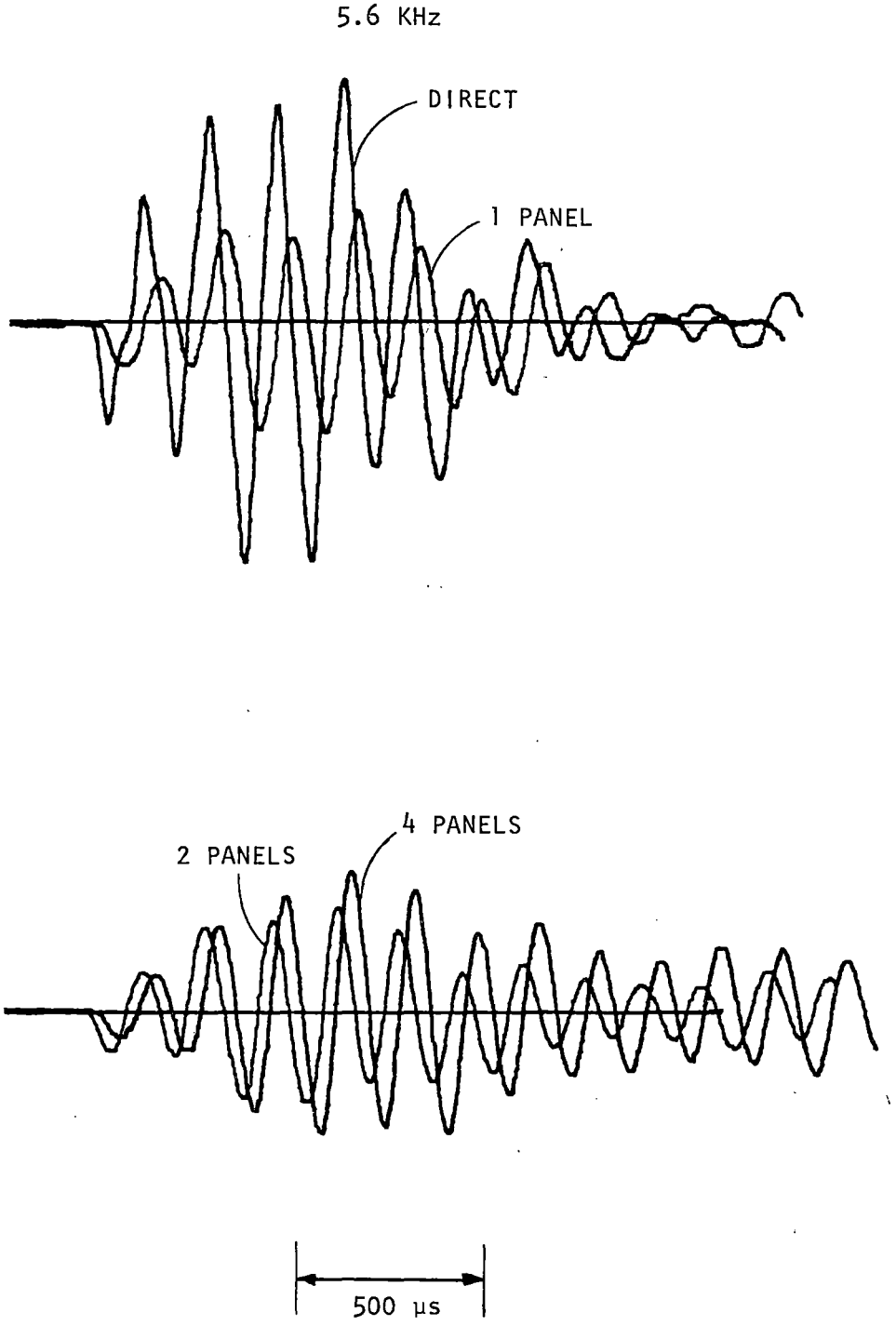

Figure 7. Example of Transmission Loss Waveforms

script refers to the number of inserted sheets. It is also important to note that the panels were clamped at the top and allowed to hang freely. No attempt was made to control the air space between the panels.

In order to limit the number of variables, the only material tested was paper. The thickness of the paper was obtained by measuring the thickness of 100 sheets and dividing by 100; this gave a thickness of $t = 6.02 \times 10^{-5}$ meters. The density of the paper was measured and found to be $\rho_p = 881$ kg/m^3. Tensile tests performed on paper coupons yielded a modulus of elasticity of $E = 53$ MPa. Other properties may now be calculated using the relation presented by Beranek [15]. The surface density of the panel is $\sigma = \rho_p t = 6.02 \times 10^{-5}$ meters, and the longitudinal wave speed is $C_L = \sqrt{E/\rho_p} = 245$ m/s. The bending stiffness of the panel is

$$B = \left(\frac{1.8\ t}{2\pi}\right)^2 \left(\frac{E}{\rho_p}\right) = 9.5 \times 10^{-7}\ \text{Nm}$$

Also note that variables subscripted with an a pertain to air.

Experimental Results

The experimental results are now compared with theory to check the reliability of the data. There are enough differences between the theory for single panels and multiple panels to warrant separate discussion.

Transmission Loss Through a Single Panel

The transmission loss data for the single panel are listed in Table I and plotted in Figure 8. The general trend is that the transmission loss increases with increasing frequency.

TABLE I

TRANSMISSION LOSS THROUGH ONE PANEL
FOR VARIOUS FREQUENCIES

Frequency (kHz)	Transmission Loss (dB)
0.6	4.7
0.9	4.2
1.1	2.6
1.8	5.0
2.2	3.5
2.8	5.4
3.2	4.6
3.7	5.4
4.5	6.7
5.1	8.0
5.6	7.7
6.3	8.3
6.6	10.2
7.8	11.7
8.8	12.0
9.1	11.8
9.5	11.4
10.2	9.8
10.9	11.7
11.0	11.4
12.3	12.4
12.5	11.8
13.4	13.2
13.6	12.9
14.4	14.0
15.2	15.3
15.6	15.4
16.2	16.6
16.7	15.9
17.3	17.8
17.7	18.4
19.1	18.4
19.5	19.7
20.1	21.9

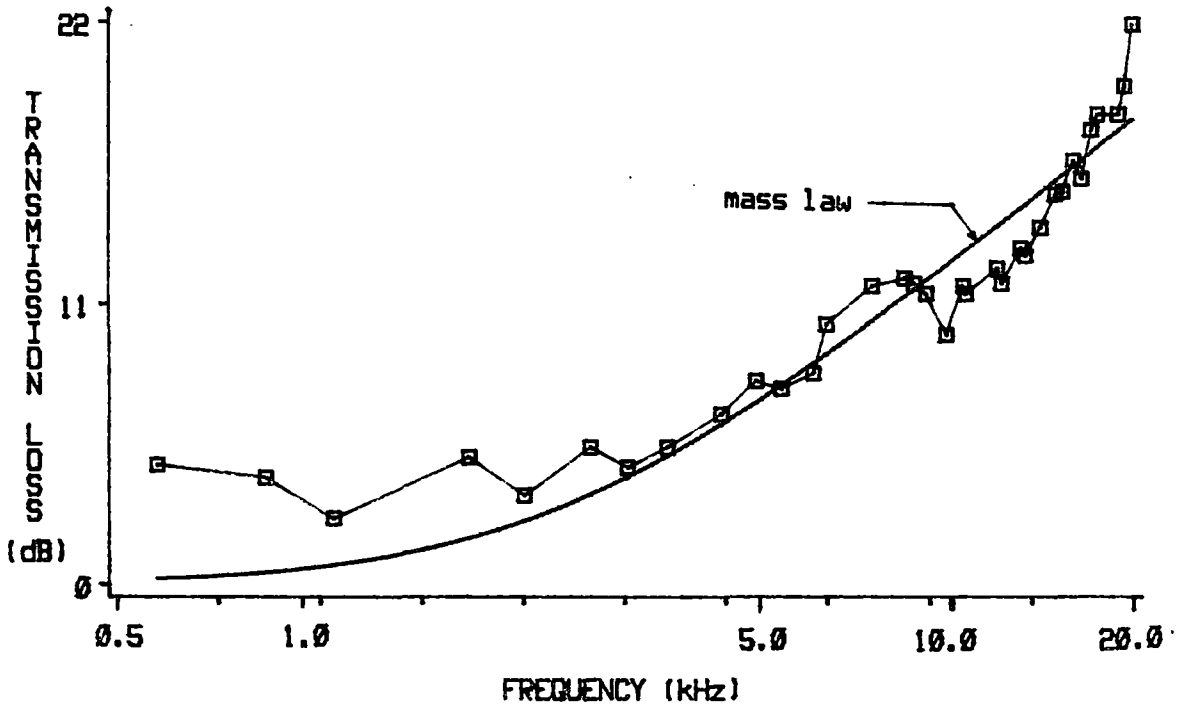

Figure 8. Transmission Loss Through One Panel

From a theoretical viewpoint, there are three frequency ranges of interest: low frequencies near the fundamental frequency of the panel, intermediate frequencies, and high frequencies near the coincidence frequency of the panel. To determine the fundamental frequency of the panel, the boundary conditions of the panel (three free edges and one fixed edge) are applied to an assumed displacement function

$$\bar{\xi}(x,z,t) = \bar{A} \sin (K_x x + \phi_x) \sin (K_z z + \phi_z) e^{j\omega t} \tag{4}$$

to yield the allowed values of K_x and K_y. Thus, the modes of free vibration are limited to

$$f_{nm} = \frac{1}{2} C_b \sqrt{\left(\frac{n - 1/2}{L_z}\right)^2 + \left(\frac{m - 1}{L_x}\right)^2} \qquad m,n = 1, 2, 3, \ldots \tag{5}$$

where C_b is the velocity of bending waves in the panel, and L_z and L_x are the panel dimensions. Since $C_b = [\omega^3 B/\sigma]^{\frac{1}{4}}$, the fundamental frequency is far lower than the range of interest due to the small bending stiffness.

The response of the panel in the intermediate frequency range is controlled by the mass. The intensity transmission coefficient for plane waves of normal incidence on a layer surrounded by air is given by Kinsler et al. [16] as

$$T_I = \frac{1}{1 + \frac{1}{4}\left(\frac{\rho_P C_L}{\rho_a C_a}\right)^2 \sin^2\left(\frac{\omega}{C_L} t\right)} \tag{6}$$

For small layer thickness (as is the case here)

$$\sin^2\left(\frac{\omega}{C_L} t\right) \simeq \left(\frac{\omega}{C_L} t\right)^2$$

The transmission loss is related to the intensity transmission coefficient by the equation

$$T.L. = 10 \log\left(\frac{1}{T_I}\right) \tag{7}$$

Substituting Equation (7) into Equation (6) yields the final result

$$T.L. = 10 \log\left[1 + \left(\frac{\omega\sigma}{2\rho_a C_a}\right)^2\right] \tag{8}$$

Equation (8) is known as the normal incidence mass law. This equation is plotted in Figure 8 with the single panel transmission loss data. Agreement is excellent.

The high frequency response is dominated by the resonant modes of the panel, in that the panel begins to radiate acoustic power. This occurs at or near the coincidence frequency f_c. Coincidence occurs when the bending wave speed in the panel is equal to the speed of sound in air. The coincidence frequency is given by

$$f_c = \frac{C_a^2}{2\pi}\sqrt{\frac{\sigma}{B}} \tag{9}$$

Carrying out this computation for the paper panels considered here yields $f_c = 4.4$ MHz, which is far beyond the frequency range of interest in this study. Price and Crocker [17] give a very thorough treatment of the transmission loss near the coincidence frequency.

Transmission Loss Through Multiple Panels

The transmission loss data for two and four panels are listed in Tables II and III and plotted in Figures 9 and 10, respectively. It can be seen from the figures that at the high frequency end, the behavior is

TABLE II

TRANSMISSION LOSS THROUGH TWO PANELS
FOR VARIOUS FREQUENCIES

Frequency (kHz)	Transmission Loss (dB)
0.6	5.4
1.1	4.9
1.9	7.3
4.4	9.9
5.6	8.2
6.3	6.2
7.8	8.0
9.0	12.8
10.2	8.2
10.9	5.0
11.0	8.2
12.5	8.6
13.6	10.5
13.9	11.7
14.5	9.9
15.2	11.7
16.9	9.6

TABLE III

TRANSMISSION LOSS THROUGH FOUR PANELS
FOR VARIOUS FREQUENCIES

Frequency (kHz)	Transmission Loss (dB)
0.6	7.9
1.1	7.1
1.9	8.2
4.4	13.2
5.6	6.6
6.3	7.2
6.4	13.6
7.8	10.0
9.0	26.4
9.1	23.1
10.2	15.5
10.9	25.8
11.0	16.3
12.5	17.1
13.6	18.2
13.9	33.2
14.5	14.9
15.2	19.4

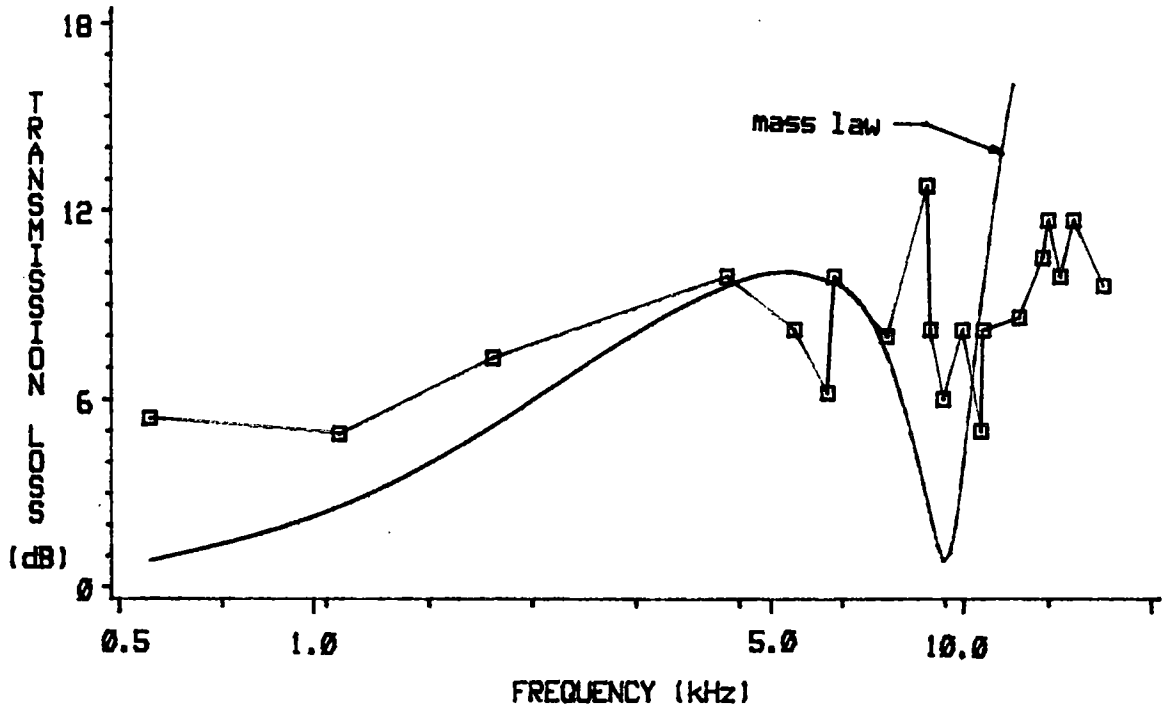

Figure 9. Transmission Loss Through Two Panels

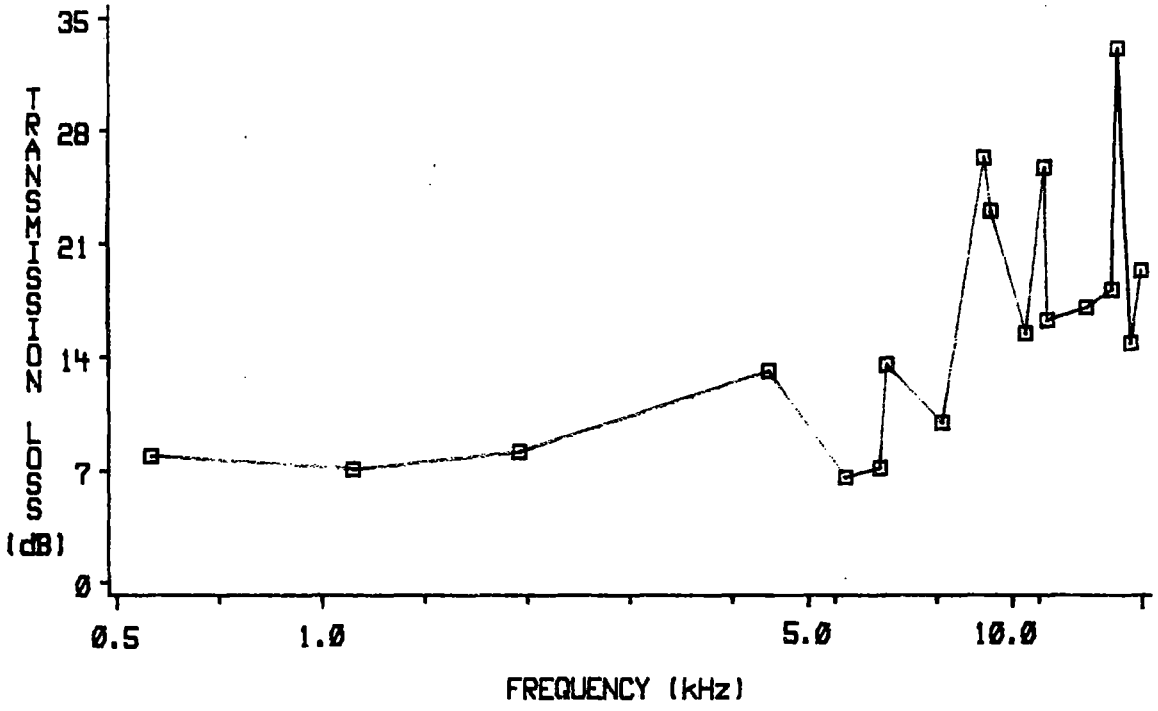

Figure 10. Transmission Loss Through Four Panels

very erratic. The low frequency range response of multiple panels is similar to the response of a single panel. If the wavelength is much larger than the air space thickness, the air acts as a soft spring which couples the panels together. The response would be governed by the fundamental frequency of the panel. This frequency is too low to be of interest here.

The air coupling of the panels holds well into the intermediate frequency range. But unlike the single panel, multiple panels exhibit a phenomenon called multiple-wall resonance. Consider the double panel system; since the panels are identical the resonant frequency is [18]

$$f_o = \frac{1}{2\pi}\sqrt{\frac{2\rho_a C_a^2}{L\sigma}} \tag{10}$$

where L is the air space thickness. This resonant frequency is also predicted by the two-panel mass law derived by Beranek and Work [19]

$$T.L. = 10 \log\left[A^2 + \left(B + A\ \frac{\omega\sigma}{\rho_a C_a}\right)^2\right] \tag{11}$$

where

$$A = \cos\left(\frac{\omega L}{C_a}\right) - \left(\frac{\omega\sigma}{\rho_a C_a}\right)\sin\left(\frac{\omega L}{C_a}\right)$$

$$B = \sin\left(\frac{\omega L}{C_a}\right) + \left(\frac{\omega\sigma}{\rho_a C_a}\right)\cos\left(\frac{\omega L}{C_a}\right)$$

Equation (11) is plotted in Figure 9 for an airspace of 2 mm. Considering the fact that the air space thickness in the experiments was probably different for each pulse and that the panels may have been in contact with each other at some point, the agreement is excellent. Note that the transmission loss is significantly reduced at the resonant fre-

quency and that Equations (10) and (11) predict exactly the same frequency. For four panels there will be three of these resonances--one given by Equation (10) and two lower ones (recall that for semi-definite systems one of the natural frequencies is zero).

In the high frequency range the point will be reached where either the wavelengths are comparable to the air space thickness or wave coincidence will occur. In either case the transmission loss will be significantly reduced. However, these frequencies are well beyond the current range of interest.

Summary

It has been shown, both experimentally and theoretically, that the transmission loss of one, two, and four paper panels is mass controlled for the frequency range 500 to 20,000 Hz. In addition, the theory shows that, due to the very low bending stiffness and small thickness of the paper, this frequency range can be extended to lower and higher frequencies. The theory also suggests that for multiple panels the air layer between the panels couples them together, resulting in resonant frequencies at which the transmission loss is significantly reduced. This was also demonstrated by the experiments. Since the main concern is actually the reflected wave and not the transmitted wave, the observation is made that a large transmission loss indicates a high reflectivity and vice versa.

CHAPTER IV

MODELING OF THE ROLL

The results of the previous chapter showed that the air layer between subsequent layers of paper act as a spring, coupling the layers together. It was thought that perhaps the same type of coupling might occur between the layers of a roll; and if this were true, the resonant frequencies would provide a measurable phenomenon. The concept of measuring the roll softness using acoustic reflections has been abandoned. Instead the solution to the problem of measuring the thickness of the entrained air is sought. Measuring the entrained air provides an instantaneous indication of roll condition, while a roll hardness measurement requires a certain amount of layers to build up before the roll quality can be determined, since roll hardness is a bulk property. Actually this may be more important. In this chapter, a model of a hard roll with one loose layer is modeled and the characteristics examined.

Model Development

The model used to describe the roll of web material with one loose layer is shown schematically in Figure 11. The chosen geometry is planar instead of cylindrical. An acoustic plane wave, originating from the left, is incident on: a single flexible panel of surface density σ, an air space of thickness L, and a semi-infinite solid of density ρ_p and acoustic propagation velocity C_p.

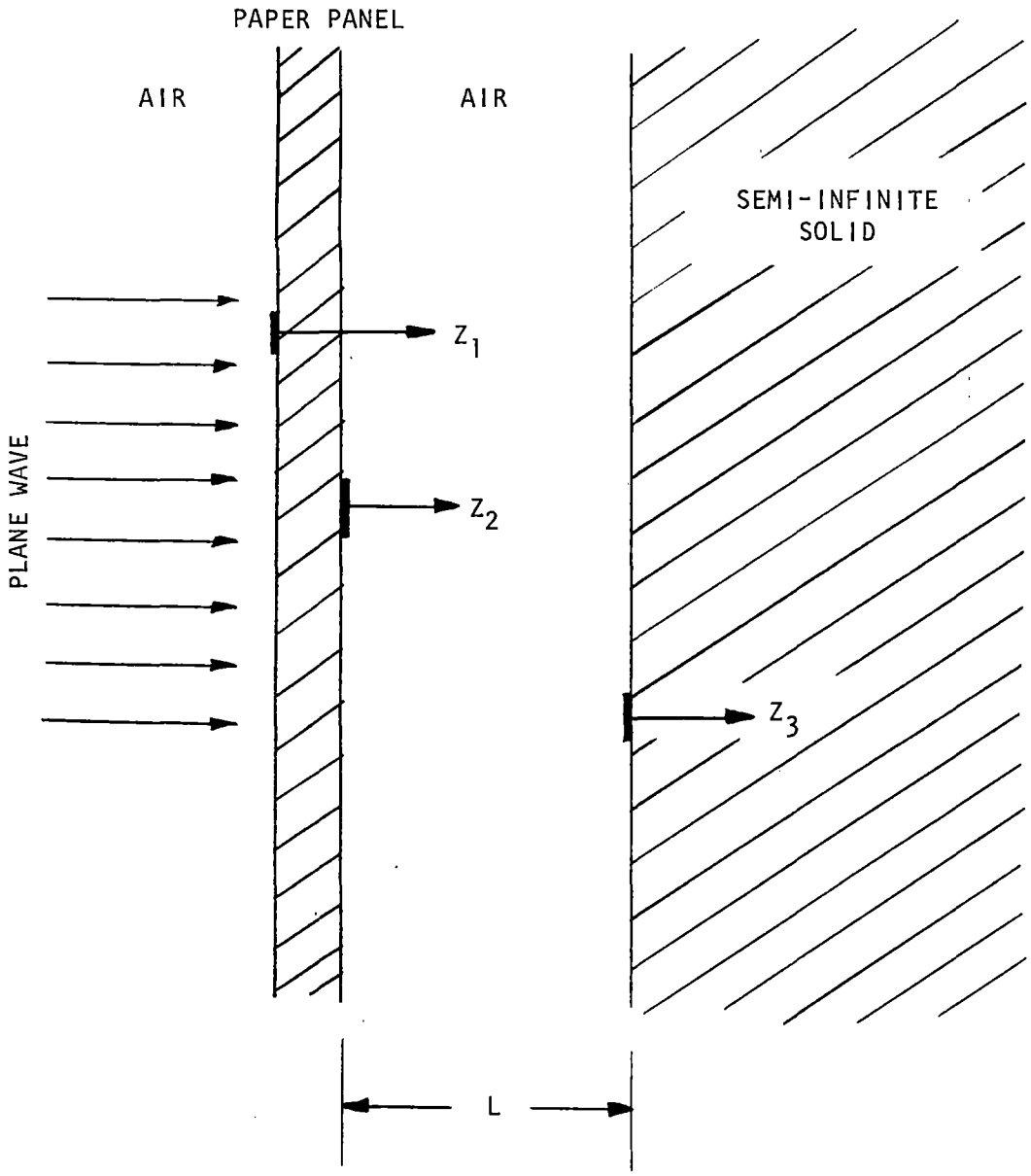

Figure 11. Model of a Roll With One Loose Layer

The acoustic impedance of the model is derived using the method presented by Beranek and Work [19]. The impedance of the model is obtained by writing the impedance each interface sees when looking to the right. This method allows the overall impedance of the model to be built up by starting at the right interface and working left. The pressure in each of the three media will be

$$P = A \cosh (bs + \psi) \tag{12}$$

where x is the distance from a terminal impedance, b is the propagation constant for the medium, and

$$\psi = \coth^{-1} \frac{\bar{Z}_t}{\bar{Z}_o} \tag{13}$$

where $\bar{Z}_o$ is the characteristic impedance on the right side of the interface in question, and $\bar{Z}_t$ is the terminal impedance. Equation (13) follows directly from the impedance relation

$$\bar{Z} = \bar{Z}_o \coth (bs + \psi) \tag{14}$$

by setting $\bar{Z} = \bar{Z}_t$ at $x = 0$.

Defining the characteristic impedance as $r = \rho c$, the impedance the third interface sees when looking right may be written as

$$\bar{Z}_3 = \rho_p C_p = r_p \tag{15}$$

With the help of Equation (14), the impedance facing right as seen from interface two is determined to be

$$\bar{Z}_2 = r_a \coth (bs + \psi) \tag{16}$$

In the air space, $x = L$, $b = j\omega/C_a$, and ψ is given by Equation (13) as

$$\psi = \coth^{-1}\left(\frac{\bar{Z}_3}{\bar{Z}_o}\right) = \coth^{-1}\left(\frac{r_p}{r_a}\right) \tag{17}$$

Equation (16) now becomes

$$\bar{Z}_2 = r_a \coth\left(\frac{j\omega L}{C_a} + \coth^{-1}\left(\frac{r_p}{r_a}\right)\right) \tag{18}$$

Expanding and simplifying, Equation (18) yields

$$\bar{Z}_2 = \frac{r_p + j r_a \tan(\omega L/C_a)}{1 + j\, r_p/r_a \tan(\omega L/C_a)} \tag{19}$$

Finally, assuming no stiffness for the panel and realizing that the velocity is continuous across the panel, the overall impedance is

$$\bar{Z}_1 = j\omega\sigma + \bar{Z}_2 \tag{20}$$

Substituting Equation (19) into Equation (20) and simplifying leads to

$$\bar{Z}_1 = \frac{r_p\left(1 + \tan^2\left(\frac{\omega L}{C_a}\right)\right)}{1 + \left(\frac{r_p}{r_a}\right)^2 \tan^3\left(\frac{\omega L}{C_a}\right)} + j\,\frac{\omega\sigma + r_a \tan\left(\frac{\omega L}{C_a}\right) + \left(\frac{r_p}{r_a}\right)^2 \omega\sigma \tan^2\left(\frac{\omega L}{C_a}\right) - \frac{r_p^2}{r_a}\tan\left(\frac{\omega L}{C_a}\right)}{1 + \left(\frac{r_p}{r_a}\right)^2 \tan^2\left(\frac{\omega L}{C_a}\right)} \tag{21}$$

Equation (21) is the impedance seen by the plane wave as it impacts the structure of Figure 11.

Characteristics of the Model

The characteristics of the model are now presented, particularly

with respect to the reflections of the plane wave. Kinsler [16] gives the intensity reflection coefficient of a plane wave normally incident on a solid of impedance $\bar{Z}$ = Re + j Im as

$$R_I = \frac{(Re = r_a)^2 + I_n^2}{(Re + r_a)^2 + I_n^2} \tag{22}$$

The impedance of Equation (21) is examined with respect to the intensity reflection coefficient of Equation (22). Frequency and air space thickness are the parameters to be varied. Since paper was the material used in this study, the properties of paper will be used in Equation (22). The surface density of the paper panel is 0.05304 kg/m^2 and the density of the semi-infinite solid in Figure 11 is the density of paper 881 kg/m^3. To obtain a good approximation of a roll of paper, the actual acoustic propagation velocity is used; this was experimentally measured by Pfeiffer [4] as 250 m/s.

The intensity reflection coefficient given by Equation (22) is plotted in Figures 12, 13, and 14 as a function of air space thickness with frequency as a parameter. The figures show that as the frequency increases, the air space thickness at which R_I reaches its minimum gets smaller. In addition, the air space thickness band over which the "dip" in the intensity reflection coefficient occurs gets smaller with increasing frequency. This explains the failure, mentioned earlier, to produce an attenuated reflection from the rolls with a loose outer ply. The frequency and air space thickness must be fairly well matched to yield an attenuated reflection. Also, the minimum intensity reflection coefficient (R_{Imin}) decreases initially for increasing frequency, reaches an absolute minimum, and then begins to increase.

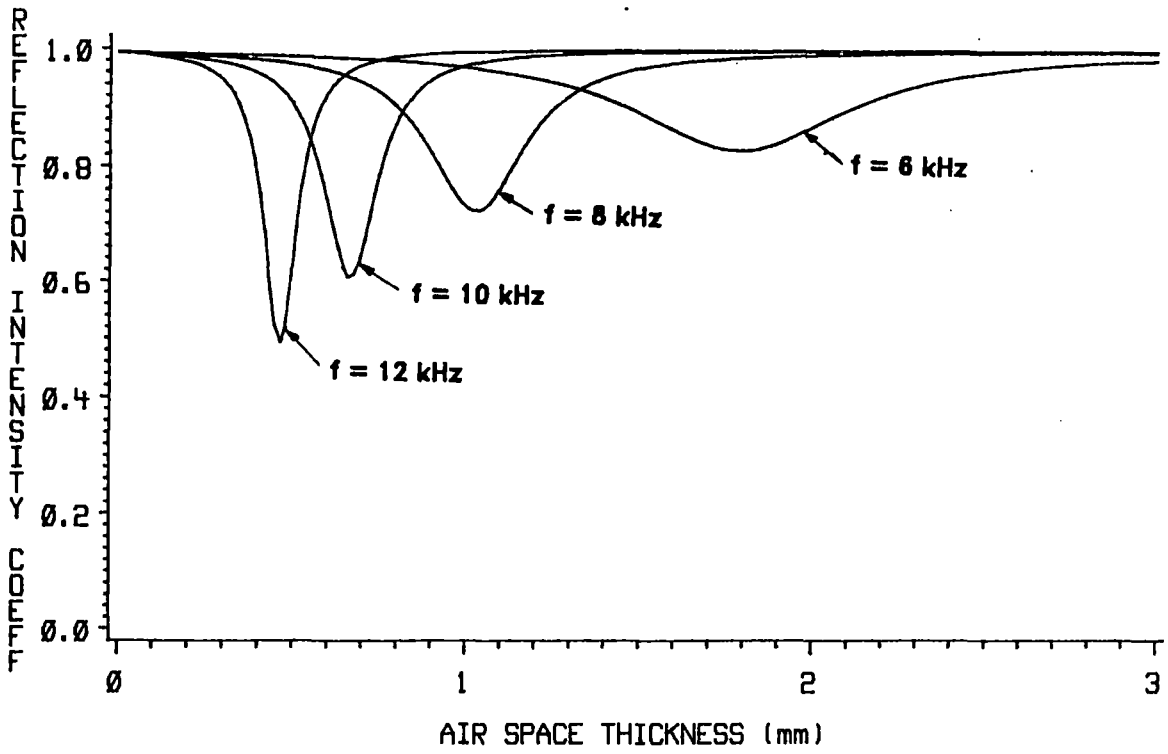

Figure 12. Plot of R_1 vs Air Space Thickness for Low Frequencies

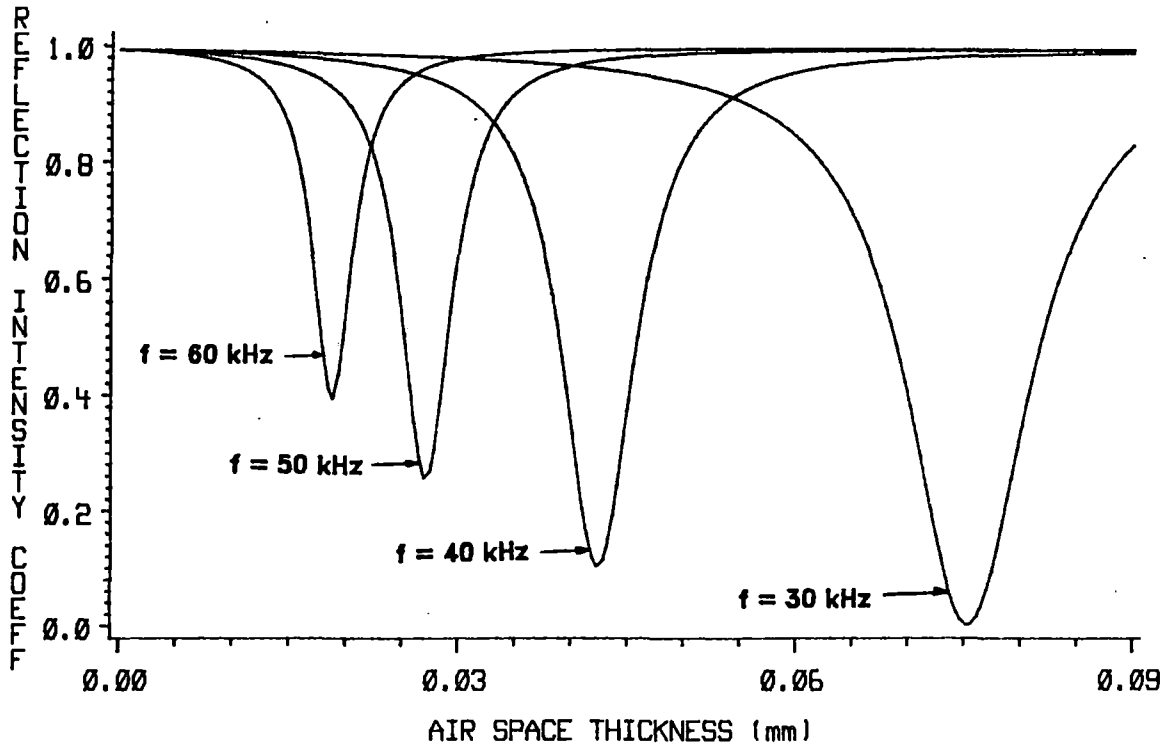

Figure 13. Plot of R_1 vs Air Space Thickness for Intermediate Frequencies

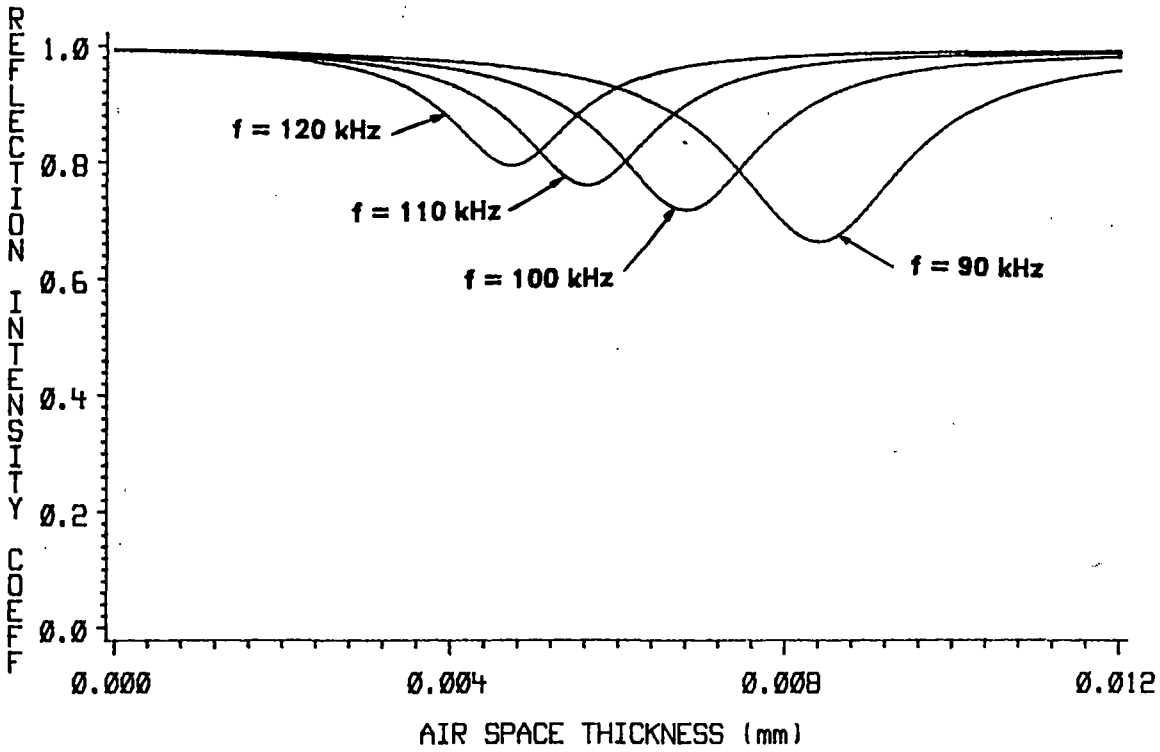

Figure 14. Plot of R_1 vs Air Space Thickness for High Frequencies

A computer program was used to numerically solve for R_{Imin} versus frequency as a function of frequency and air space thickness. A plot of R_{Imin} versus frequency is shown in Figure 15, and a plot of the air space thickness at which R_{Imin} occurs (denote this the critical air gap) as a function of frequency is shown in Figure 16. From the figures it can be seen that the minimum value of R_I is reached at a frequency of 28 kHz, and a critical air gap of 0.0865 mm. Recall that the thickness of the paper is 0.06 mm. In order to detect an air space thickness of 1/10, using a reflection technique would require a frequency of 106 kHz. Figure 16 also shows that past a frequency of about 15 kHz, significant increases in frequency are needed to produce smaller critical air gaps.

Further analysis of the model proves that a resonance phenomenon causes the intensity reflection coefficient to reach its minimum values, since the reactance goes to zero. Figures 17 and 18 show the magnitude and phase, respectively, of the impedance of the model (Equation (21)) as a function of frequency for three values of the space thickness. Note that for each of the three values of L, the reactance is zero and the resistance is minimum at the same frequency; at this frequency the value of L corresponds to the critical air gap. Furthermore, Figure 16 may be considered as the locus of points in the air space thickness-frequency plane at which the minimum value of the intensity reflection coefficient occurs.

A relation may be derived for this resonant frequency by multiplying Equation (10) by $1/\sqrt{2}$ to give

$$f_o = \frac{1}{2\pi}\sqrt{\frac{a\,C_a^2}{L\sigma}} \tag{23}$$

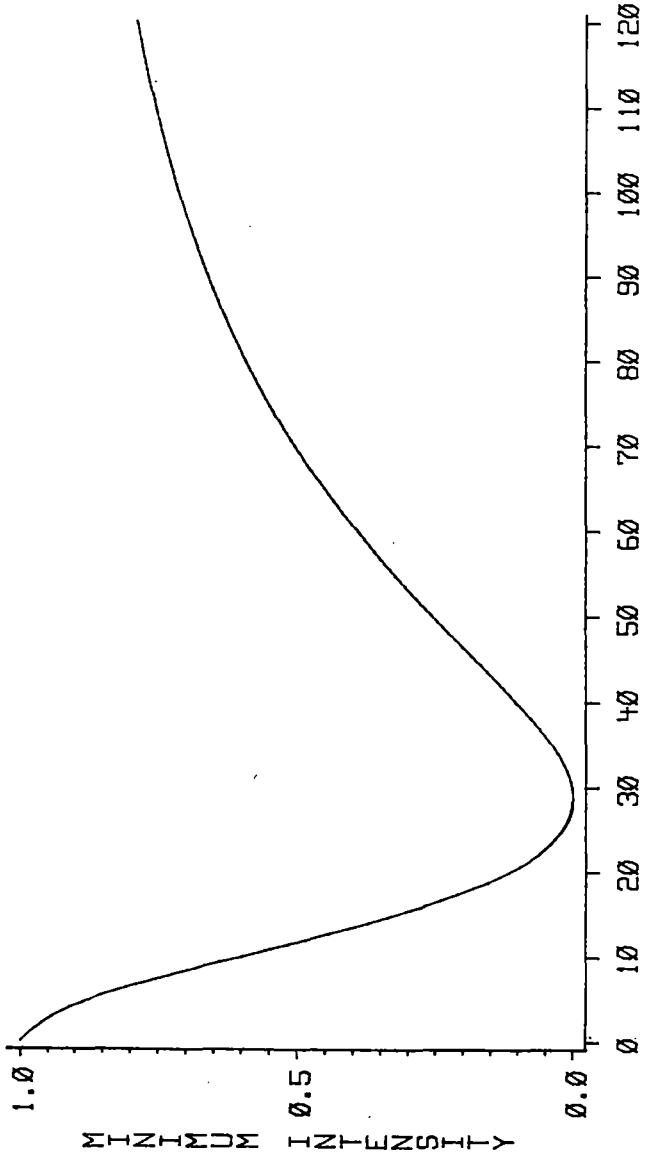

Figure 15. Plot of R_{Imin} vs Frequency

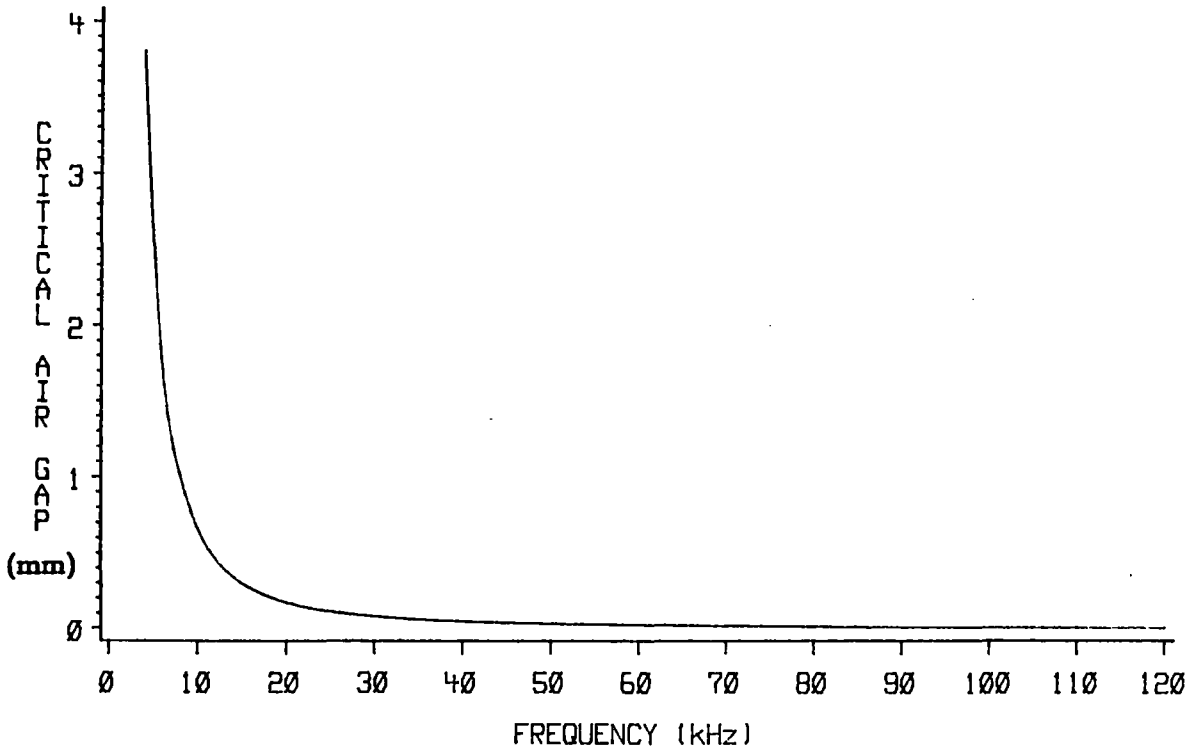

Figure 16. Plot of the Critical Air Gap vs Frequency

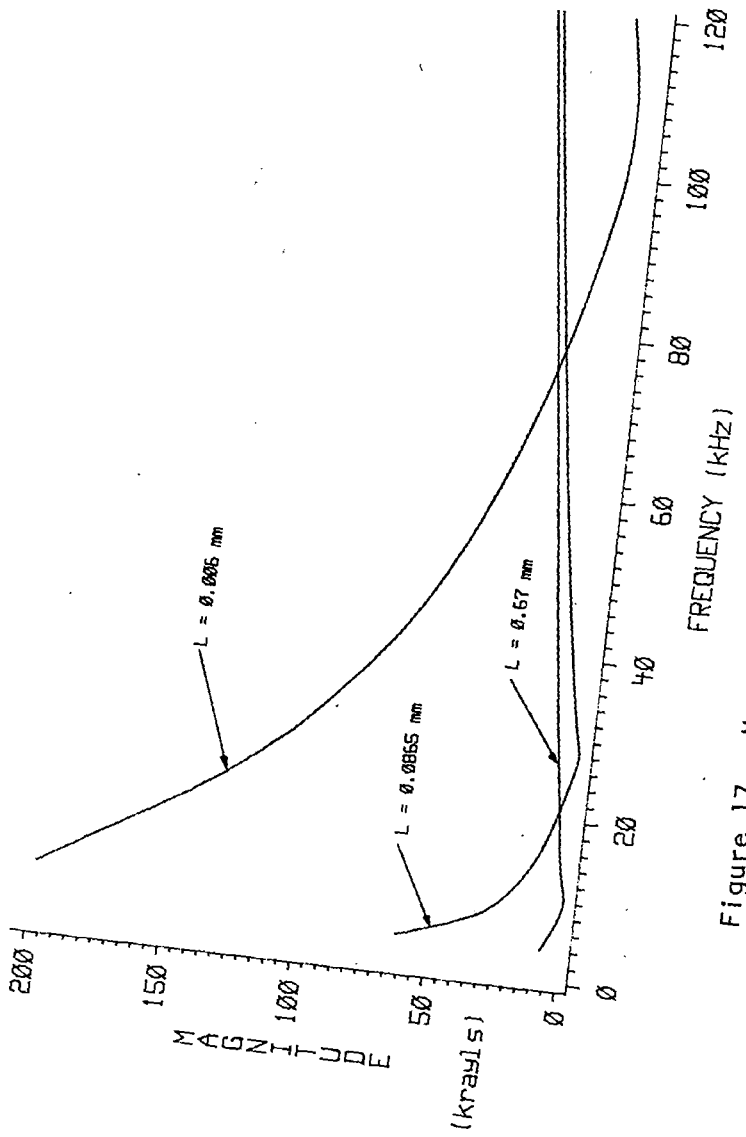

Figure 17. Magnitude of the Impedance vs Frequency

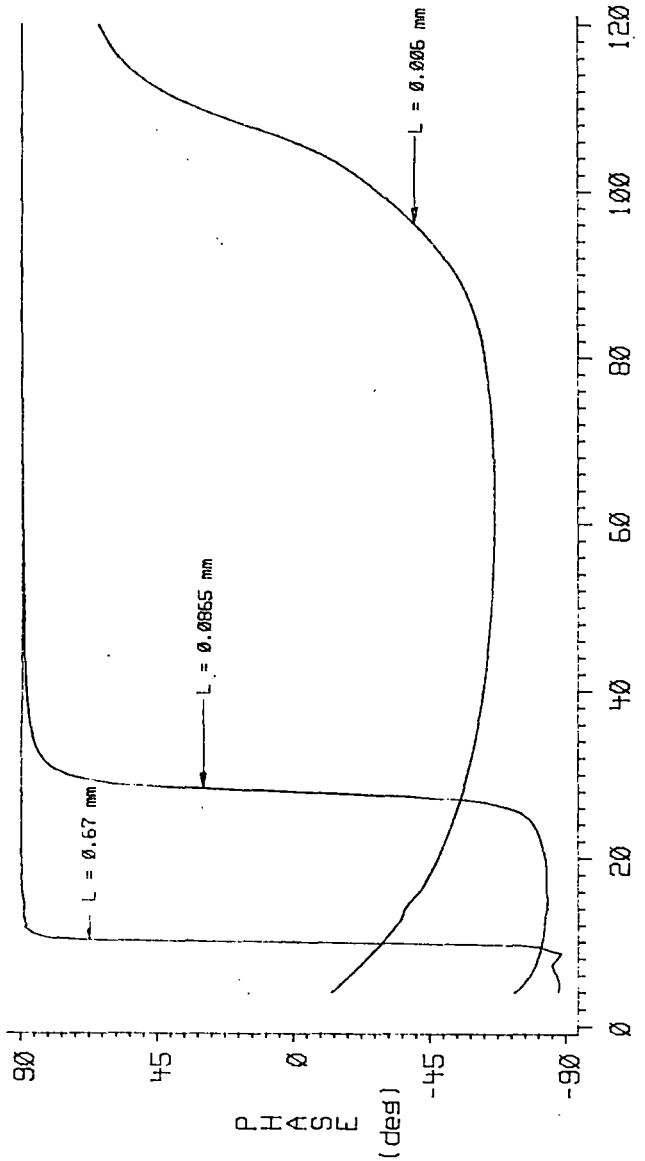

Figure 18. Phase of the Impedance vs Frequency

This is because the model described here is the definite system corresponding to the semi-definite system consisting of two identical panels separated by an air space. When one of the masses of a semi-definite system is held fixed, the natural frequency decreases by a factor of $1/\sqrt{2}$.

CHAPTER V

TESTS ON A PAPER ROLL

The model presented in Chapter IV appears very simple when compared to the actual situation. The two assumptions concerning the use of planar as opposed to cylindrical geometry and plane waves as opposed to spherical waves are the most critical. However, the validity of these assumptions improves with increasing frequency because of the increasing number of wavelengths between the source and point of impact. In this chapter experiments performed to test the model of the previous chapter are described.

Experimental Procedure

The measurement system used in this series of tests is shown in Figure 19. The geometry was chosen to minimize the effect of attenuation of the acoustic signal in air, allow sufficient separation of the direct and reflected pulses, and keep the angle of incidence of the incident wave as small as possible. The speaker and microphone were placed under the roll so that the acoustic waves impacted the freely hanging outer ply. The web material used was paper.

The reflected signals were recorded as the air gap was increased from zero. The roll was positioned so that the end of the outer ply was at the top of the roll. The edge was held tightly to obtain an air space thickness of zero, and a reflection was recorded. The edge was then

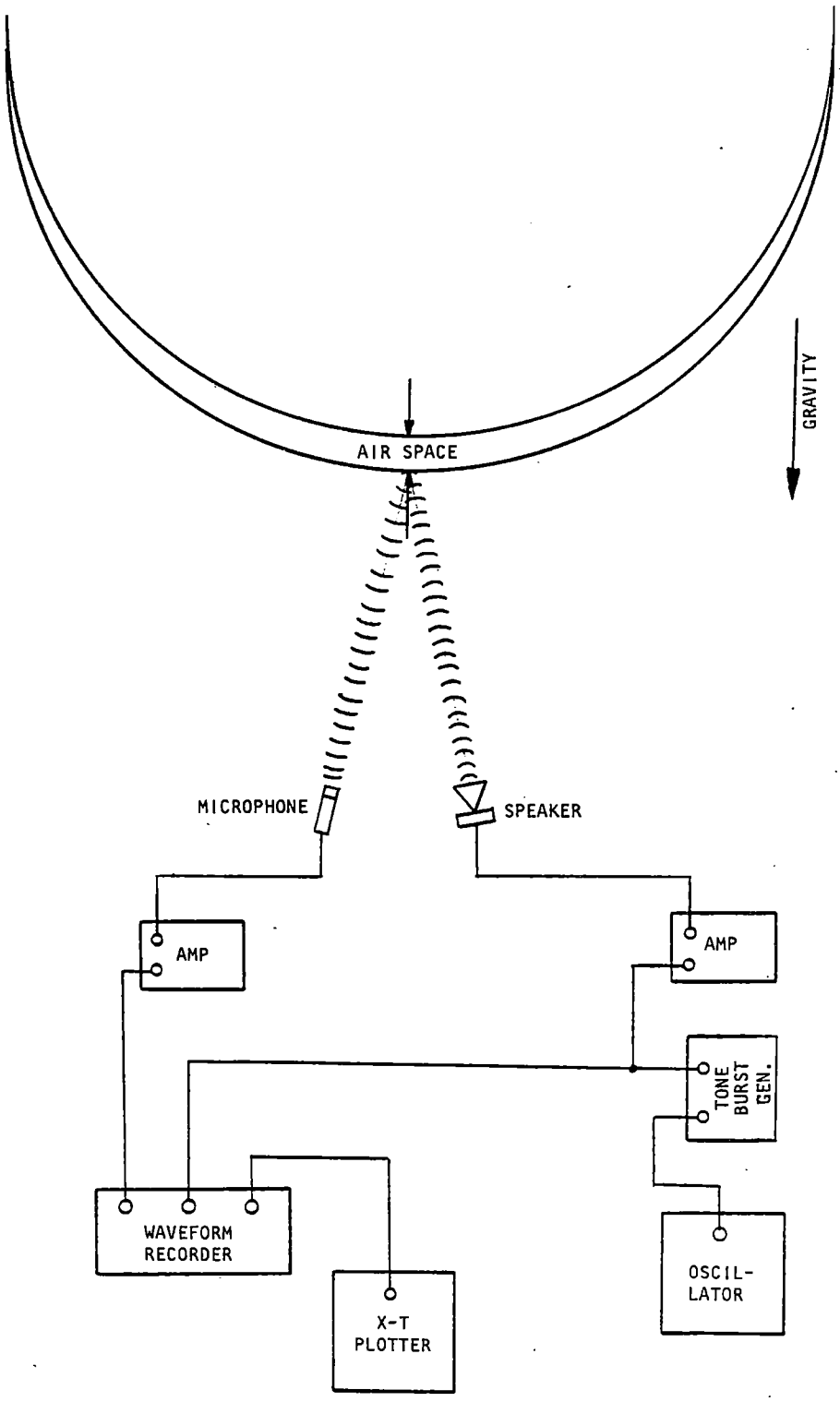

Figure 19. System Used to Measure Reflection Ratio

advanced in steps of half a millimeter and reflections were recorded at each step. The amplitudes of the last three cycles were averaged (the pulse train was four cycles long). Using the average amplitude of the reflected signal at zero air space thickness as a basis, a reflection ratio may be defined as

$$R = \frac{\text{Average Amplitude at } L = X}{\text{Average Amplitude at } L = 0} \tag{24}$$

Experimental Results

The reflection ratios obtained for frequencies of 6 and 10 kHz are listed in Tables IV and V, and plotted in Figures 20 and 21. The intensity reflection coefficient given by Equation (22) is also plotted in Figures 20 and 21 for comparison with the model. Note that R and R_I are not equivalent quantities. The important result is that R and R_I reach their minimum values at about the same value of the air space thickness. A reflection ratio for the model would be proportional to the square root of the intensity reflection coefficient. Thus, the magnitude of the reflection ratio predicted by the model is smaller than the experimentally measured reflection ratio.

Conducting this experiment at higher frequencies than 10 kHz would require a much more sophisticated setup. From Figure 12, it can be seen that the air space thickness band over which dip in the R_I curve occurs is only about a third of a millimeter at 12 kHz. This is in the range of uncertainty in the current experimental setup.

Summary

Considering how simple the model is, it is extremely encouraging

TABLE IV

REFLECTION RATIOS FOR VARIOUS AIR SPACE WIDTHS (FREQUENCY = 6 KHZ)

R (mm)	R Run 1	R Run 2
0.00	1.00	1.00
0.32	0.99	0.99
0.64	0.97	0.96
0.95	0.90	0.93
1.27	0.80	0.88
1.59	0.68	0.55
1.90	0.51	0.49
2.22	0.55	0.56
2.53	0.57	0.61
2.85	0.58	0.58
3.16	0.57	0.59

TABLE V

REFLECTION RATIOS FOR VARIOUS AIR SPACE WIDTHS (FREQUENCY = 10 KHZ)

L (mm)	R Run 1	R Run 2
0.00	1.00	1.00
0.32	0.91	0.86
0.64	0.74	0.61
0.95	0.95	0.85
1.27	1.07	1.00
1.59	1.16	1.12
1.90	1.23	1.20
2.22	1.25	1.22
2.53	1.27	1.25

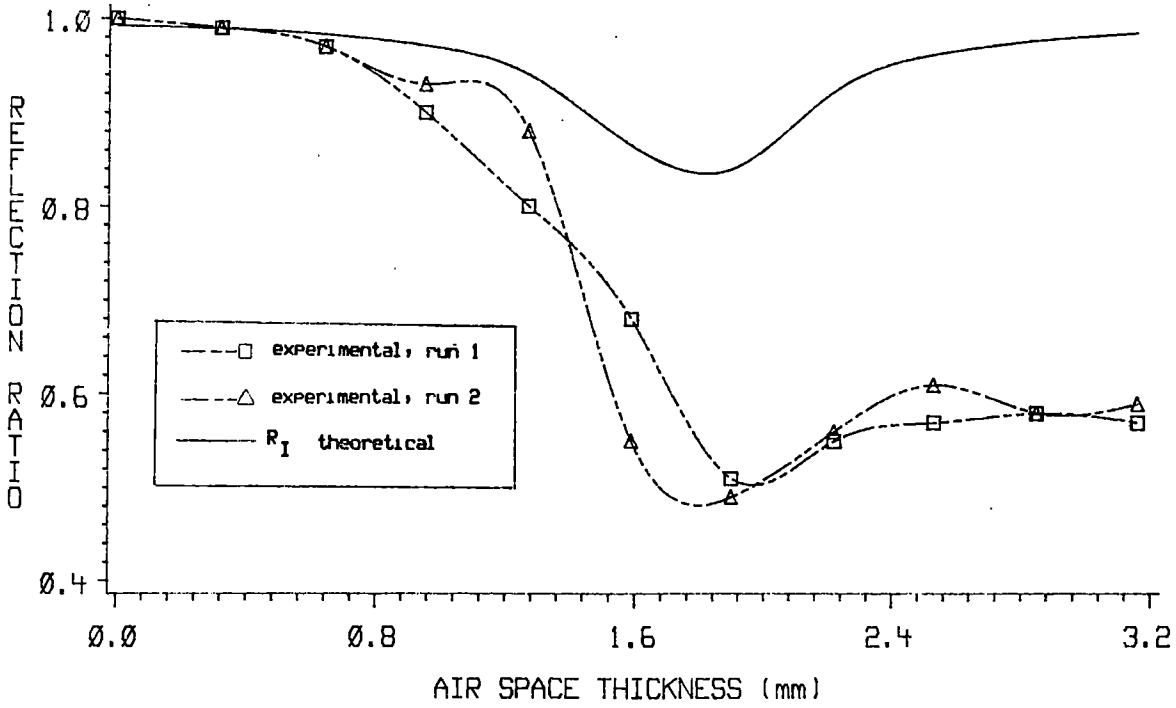

Figure 20. Comparison of Experimental Reflection Ratio With the Intensity Reflection Coefficient at 6 kHz

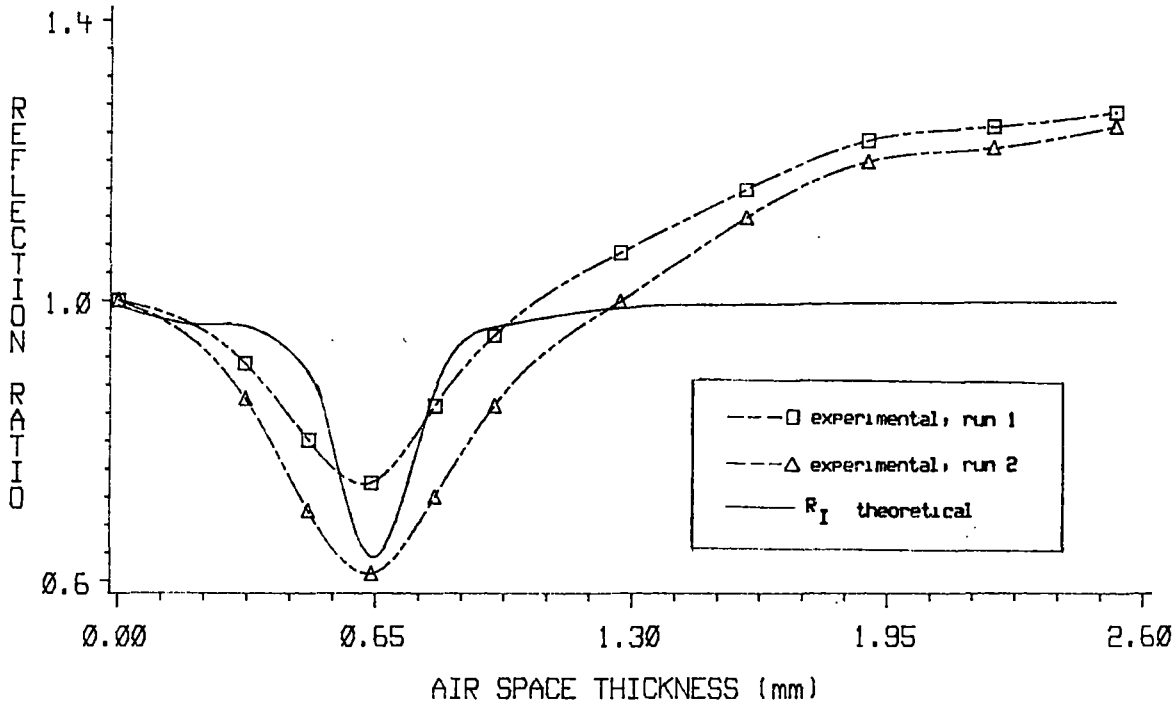

Figure 21. Comparison of Experimental Reflection Ratio With the Intensity Reflection Coefficient at 10 kHz

that it was able to predict the air space thickness at which the reflection occurred. However, the failure of the model to predict the correct magnitude of the reflection ratio is somewhat discouraging.

CHAPTER VI

CONCLUSIONS

The objective of this study was to develop a method by which roll hardness could be measured while the roll was being formed. Two different systems were investigated. One involved inputting a force impulse into the roll and monitoring the response with respect to the force and acceleration. This method requires contact with the roll. The second technique involved using acoustic pulses reflected from the roll to measure the roll hardness. This method does not require contact with the roll, and this is where the need is most evident.

Conclusions Regarding the Mechanical Impedance Method

The mechanical impedance method yielded three different variables that can be used to indicate roll hardness: the ratio of the acceleration to the duration time, the slope of the mechanical impedance curve, and the position of the peak in the frequency spectrum of the mechanical impedance curve. The most promising of the three is the acceleration-duration time ratio. This variable provides the possibility of greater resolution than the other two variables. From the standpoint of ease of computation it would yield a hardness reading faster than the other two, thus allowing a faster sampling rate. In addition, the force need not be measured. This allows for one channel acquisition

and improves accuracy because accelerometers are less sensitive to transverse loading than force transducers of the type used in this study.

Measurement of the mechanical impedance of the roll is also promising. However, the computations required to achieve the result are more exhaustive. Since the force, as well as the acceleration, are being measured, a special tip for the force transducer should be designed to reduce the transverse load caused by the sliding friction between the tip and the roll. The frequency domain variable is the least desirable of the three. Since the Fourier Transform of the mechanical impedance must be calculated, a microprocessor is almost mandatory. In addition, the resolution is much poorer. All three of these variables would require comparison to a standard in order to make a decision about the roll hardness, and the roll hardness readings would be relative to this standard.

Conclusions Regarding the Acoustic Method

Development of the acoustic method turned out to be much more difficult than originally anticipated. In fact, it appears doubtful that a method to measure the hardness of a roll based on acoustic reflections can be developed. Even in very soft rolls the layers of web material are in contact at many points. This provides too many flanking paths for the acoustic wave to follow in order to obtain resonance.

It appears very likely that an acoustic reflection method can be developed to measure the amount of entrained air. This could provide the operator with an indication that something is malfunctioning. In some respects, measuring the amount of entrained air may be superior to measuring roll hardness. In a roll hardness measurement, a certain amount of layers will have to be wound in a soft state before detection

of the softness could be indicated. Measuring entrained air provides the possibility of layer-by-layer monitoring of the roll condition. Of course, the transducer would have to be placed so that it can take a reading before the air exits the end of the roll.

Recommendations for Future Studies

The mechanical measurement system has proven to be very successful. A prototype is ready to be constructed and tested. It is suggested that the peak acceleration-time duration method be employed. The pressure wave anomaly also needs to be investigated.

Future studies of the acoustic method must first determine if the intensity reflection coefficient behaves as predicted by the model at high frequency. Thus, some means of obtaining very small air space thicknesses must be devised and ultrasonic equipment with 100 kHz plus operating range. Only after this step has been completed and the phenomenon verified should factors concerning implementation be addressed.

REFERENCES

[1] Frye, K. G. "New Winding Methods and Basic Winding Parameters." Tappi (May, 1985), p. 66.

[2] "Test for Determining Roll Hardness." Tappi, Vol. 45, No. 12 (December, 1962), pp. 126A.

[3] "Hardness of Paper Rolls." Tappi, Vol. 54, No. 7 (July, 1971), p. 1177.

[4] Pfeiffer, J. D. "Internal Pressures in a Wound Roll of Paper." Tappi, Vol. 49, No. 8 (August, 1966), p. 342.

[5] Welp, E. G., and H. Schoenmeier. "Improving Roll Structure--a Research Report." Tappi (April, 1984), p. 70.

[6] Monk, D. W., W. K. Lautner, and J. F. McMullen. "Internal Stresses Within Rolls of Cellophane." Tappi, Vol. 58, No. 8 (August, 1975), p. 152.

[7] Frye, K. G. "Winding Variables and Their Effect on Roll Hardness and Roll Quality." Tappi, Vol. 50, No. 7 (July, 1967), p. 81A.

[8] Laumer, E. P. "Minimizing 'Wound-In' Paper Defects Within Shipping Rolls." Tappi, Vol. 49, No. 12 (December, 1966), p. 127A.

[9] Eriksson, L. G., C. Lydig, and J. A. Viglund. "Measurement of Paper Roll Density During Winding." Tappi (January, 1983), p. 63.

[10] McDonald, J. D., and W. R. Farrell. "Winder Optimization Using an On-Line Microcomputer." Pulp and Paper Canada, Vol. 86, No. 9 (1985), p. T250.

[11] Duff, I. L. "Unique Tester Improves Quality." Canadian Chemical Processing (April, 1977), p. 30.

[12] Quint, R. J. "Measurement and Control of Paper Roll Condition." Tappi, Vol. 51, No. 9 (September, 1968), p. 373.

[13] Advertisement. Tappi, Vol. 51, No. 12 (December, 1968), p. 175A.

[14] Doebelin, E. O. Measurement Systems Application and Design. 3rd ed. New York: McGraw-Hill Book Company, 1983.

[15] Beranek, L. L. Noise Control. McGraw-Hill Book Co., 1971.

[16] Kinsler, L. E. et al. Fundamentals of Acoustics. 3rd ed. John Wiley and Sons, 1982.

[17] Croker, M. J., and A. J. Price. "Sound Transmission Using Statistical Energy Analysis." Journal of Sound and Vibration, Vol. 9, No. 3 (1969), p. 469.

[18] Beranek, L. L. Noise Reduction. New York: McGraw-Hill Book Company, 1960.

[19] Beranek, L. L., and G. A. Work. "Sound Transmission Through Multiple Structures Containing Flexible Blankets." J. Acous. Soc. Am., Vol. 19 (1947), p. 419.

VITA

Paul O. Padgett

Candidate for the Degree of

Master of Science

Thesis: ROLL HARDNESS MEASUREMENT

Major Field: Mechanical Engineering

Biographical:

Personal Data: Born in St. Louis, Missouri, July 14, 1958, the son of Rev. and Mrs. Stanley D. Padgett. Married Sherri A. Jacobs on August 16, 1978, in Cyril, Oklahoma.

Education: Graduated from Apache High School, Apache, Oklahoma, in May, 1976; received the Bachelor of Science in Mechanical Engineering degree from Oklahoma State University in 1985; completed requirements for the Master of Science degree at Oklahoma State University in December, 1986.

Professional Experience: Teaching and Research Assistant, School of Mechanical and Aerospace Engineering, Oklahoma State University, Stillwater, Oklahoma, 1985-1986.

Professional Organizations: Pi Tau Sigma, American Society of Mechanical Engineers, National Society of Professional Engineers.